Title: Transitioning from microsatellites to SNP-based microhaplotypes in genetic monitoring programs: lessons from paired data spanning 20 years.

Running title: Marker transition in genetic monitoring

Authors: Megan J. Osborne*, Guilherme Caeiro-Dias, Thomas F. Turner

Affiliations: Department of Biology and Museum of Southwestern Biology, MSC 03-2020, University of New Mexico, Albuquerque, New Mexico, 87131, USA.

*Corresponding author; Email: mosborne@unm.edu; ORCID ID: 0000-0002-0978-2905

Keywords: Demography, genetic effective population size, multi-locus heterozygosity, rapid evolution, inbreeding, long-term monitoring, RAD-seq

Abstract

Many long-term genetic monitoring programs began before next-generation sequencing became widely available. Older programs can now transition to new marker systems usually consisting of 1000s of SNP loci, but there are still important questions about comparability, precision, and accuracy of key metrics estimated using SNPs. Ideally, transitioned programs should capitalize on new information without sacrificing continuity of inference across the time series. We combined existing microsatellite-based genetic monitoring information with SNP-based microhaplotypes obtained from archived samples of Rio Grande silvery minnow (*Hybognathus amarus*) across a 20-year time series to evaluate point estimates and trajectories of key genetic metrics. Demographic and genetic monitoring bracketed multiple collapses of the wild population, and included cases where captive-born repatriates comprised the majority of spawners in the wild. Even with smaller sample sizes, microhaplotypes yielded comparable and in some cases more precise estimates of variance genetic effective population size, multilocus heterozygosity and inbreeding compared to microsatellites because many more microhaplotype loci were available. Microhaplotypes also recorded shifts in allele frequencies associated with population bottlenecks. Trends in microhaplotype-based inbreeding metrics were associated with the fraction of hatchery-reared repatriates to the wild, and should be incorporated into future genomic monitoring. Although differences in accuracy and precision of some metrics were observed between marker types, biological inferences and management recommendations were consistent.

Introduction

Genetic monitoring quantifies trajectories of individual- and population-level metrics that include heterozygosity, gene diversity and genetic effective population size (N_e) over contemporary time series (Schwartz et al. 2007). Tracking these metrics facilitates adaptive and evolutionary-cognizant management. For the past three decades, microsatellites were the workhorse for genetic monitoring programs (e.g., Koelewijn et al. 2010; Beatty and Provan 2014; Dowling et al. 2014). Long-term monitoring programs are now transitioning to next-generation high-throughput genomic approaches based on single-nucleotide-polymorphisms (SNPs) and microhaplotypes (i.e., multiple SNPs haplotyped at the same locus); raising questions about continuity and consistency across the time series as well as the relative accuracy, precision and comparability of metrics estimated with different genetic marker classes. The transition process also offers opportunities to adjust metrics and analytical procedures to better capitalize on whole-genome screening, preferably without loss of information. Microsatellite panels typically represent few loci and a small fraction of the genome, but often exhibit high rates of evolution and many distinct alleles per locus. High-throughput protocols generate SNP datasets that include numerous loci (often > 1000) that are widespread throughout the genome, but possible allelic states at each locus is limited. Next-generation sequencing typically identifies multiple SNPs on a single DNA fragment but to avoid issues with linkage, only a single SNP per fragment is retained (O'Leary et al. 2021). However, SNPs found on the same fragment can be kept as multi-allelic microhaplotypes to increase power for estimating key metrics (Baetscher et al. 2017). Increased power may be especially important for rare and endangered species with depleted genetic variation. What do differences between marker types portend for comparative

64 inferential power and, in the case of conserved populations, recommendations based on
65 monitoring made to resource managers?
66 Performance of microsatellites and other types of markers (biallelic SNPs,
67 microhaplotypes) has been evaluated in the context of spatial patterns of genetic variation, for a
68 variety of organisms, e.g., threespine stickleback (*Gasterosteus aculeatus*; DeFaveri et al. 2013),
69 bighorn sheep (*Ovis canadensis;* Miller et al. 2014), brown trout (*Salmo trutta*; Lemopoulos et
70 al. 2018), northern pike (*Esox lucius;* Sunde et al. 2020) and walleye (Bootsma et al. 2020). The
71 consensus is that marker types recovered similar patterns of broad-scale population structure, but
72 the relative performance of different marker types is context dependent (i.e., number of loci,
73 alleles, etc.). We are not aware of any study that explicitly compares key metrics across marker
74 types over time to evaluate trends in genetic diversity and effective size, even though temporal
75 studies are the foundation of genetic monitoring.
76 At the individual-level, some studies reported weak correlations of estimates obtained
77 from microsatellite and SNP data across metrics of relatedness, individual-level heterozygosity,
78 parentage, and population diversity (e.g., Fischer et al. 2017; DeFaveri et al. 2013). In most
79 cases, this is attributed to heterogeneity across the genome that may weaken correlations between
80 markers. Chakraborty (1981) showed that individual heterozygosity estimated from a small
81 number of molecular markers does not adequately represent genome-wide heterozygosity
82 (GWH) especially in the absence of identity disequilibrium (ID, i.e., non-random associations of
83 genotypes between loci; DeWoody and DeWoody 2005; Ljungqvist et al. 2010). For correlations
84 between genome-wide heterozygosity and diversity, populations must display ID (Ljungqvist et
85 al. 2010), without which, all loci within the genome will be heterozygous or homozygous
86 independently of each other (Szulkin et al. 2010). Identity disequilibrium occurs when there are

87 some consanguineous matings in the population (Bennett and Binet 1956; Ohta and Cockerham
88 1974) and ID can be used as a proxy for inbreeding (Miller et al. 2014). Population bottlenecks
89 and genetic drift, as a cause and consequence of small population size, lead to matings between
90 related individuals resulting in ID. Likewise, admixture can result in temporary ID because
91 individuals with ancestors from divergent populations are outbred, relative to individuals
92 originating from a shared ancestral population.
93 Importantly, genetic monitoring potentially provides real-time insight into the
94 relationship between heterozygosity and fitness (i.e., heterozygosity fitness correlation [HFC]),
95 including variation in reproductive success. Within populations, variation in inbreeding affects
96 genome-wide genotypic variation among individuals and causes subsequent fitness differences
97 among them (Sin et al. 2021). Studies measuring HFC are conducted to detect evidence of
98 inbreeding depression which can compromise population viability and conservation efforts (e.g.,
99 Hoffman et al. 2014; Townsend and Jamison 2013). Until recently, microsatellites were the
100 marker of choice for genetic monitoring and HFC studies due to their high variability and
101 minimal development costs. However, ascertainment bias caused by selecting only the most
102 polymorphic microsatellite loci results in reduced sensitivity for assessing genome-wide genetic
103 diversity (Väli et al. 2008) while the small number of microsatellite loci typically employed
104 limits power to detect inbreeding (Szulkin et al. 2010). Furthermore, estimates of inbreeding and
105 individual heterozygosity obtained from few loci are poorly correlated under most realistic
106 situations (Balloux et al. 2004; Miller and Coltman 2014). Moreover, microsatellite datasets are
107 often replete with missing data, null alleles and scoring errors that impact some population-level
108 metrics, most notably F_{IS} (e.g., David et al. 2007) and genetic effective population size (Marandel
109 et al. 2020). SNPs appear to improve accuracy and precision of GWH estimates and inbreeding

(Hoffman et al. 2014; Sin et al. 2021). Yet, although there are numerous molecular-based surrogates for inbreeding (e.g., realized individual inbreeding [F], internal relatedness [IR], multilocus heterozygosity [MLH] and *g2*; Table 2), these are not typically measured in genetic monitoring programs. As monitoring programs begin to transition toward genomic scale data, uncertainties remain regarding the utility of these alternate statistics related to inbreeding.

Simulation studies offer some guidance on the comparative sensitivity of microsatellites and biallelic SNPs to detect population declines over time, and under different demographic scenarios and sampling schemes at conservation-relevant timescales (Hoban et al. 2014). Data from real populations are scarce (but see Lehnert et al. 2018) and the relative power of microhaplotypes has not been investigated to our knowledge. A long-term genetic and demographic monitoring program of the Rio Grande silvery minnow (*Hybognathus amarus*) provides an opportunity to conduct a side-by-side comparison between microsatellites and microhaplotypes obtained from representative archived samples. Over the last 70 years, this species has contended with habitat changes associated with river fragmentation, dewatering, and flood control that have caused significant range contraction (Platania 1993). Since listing under the Endangered Species Act in 1994 (U.S. Fish and Wildlife Service 1994), droughts and water extraction have caused periodic population collapses associated with recruitment failure (Archdeacon and Reale 2020; Archdeacon et al. 2020). A full-scale captive breeding and augmentation program began in 2002-2003 (U.S. Fish and Wildlife Service 2018) and progeny from this program sometimes comprise the majority of the spawning stock in the wild. Population bottlenecks and genetic drift associated with augmentation are expected to impact GWH (Szulkin et al. 2010) and genetic monitoring of the population should reveal signatures of these events in the genome provided genetic markers have sufficient power.

Like other conservation programs, maintenance of genome-wide diversity and adaptive potential are major tenets of the Rio Grande silvery minnow conservation program, but whether findings from small panels of microsatellites accurately reflect genome-wide patterns have been widely debated (e.g., Miller et al. 2014). Results obtained from microhaplotypes also must be directly comparable to previous results to preserve the continuity and comparability of the time series. Using a genetic monitoring time series spanning two decades we: (i) summarized patterns of genetic variation, divergence and effective size using microsatellites and microhaplotypes, (ii) assessed whether measures of population genetic diversity, individual diversity, divergence and contemporary genetic effective population size were correlated between microsatellites and microhaplotypes; and (iii) assessed whether other metrics (i.e., MLH, IR, g_2) estimated from genomic data, would be a valuable addition to the genetic monitoring programs. Leveraging the power of genomic data could provide additional insight not afforded by microsatellite markers, thereby strengthening the value of genetic monitoring to ongoing adaptive management of the species.

Methods

Demographic Monitoring Data and Modeling

Rio Grande silvery minnow is a small-bodied, short-lived (Horwitz et al. 2018) cyprinid that was widely distributed in the Rio Grande from northern New Mexico to the Gulf of Mexico, and in the Pecos River from northern New Mexico to the confluence of the Rio Grande in Texas (Pflieger 1980). A remnant population persists in the Rio Grande in New Mexico extending from downstream of Cochiti Dam to Elephant Butte Reservoir (Bestgen and Platania 1991). This river reach is referred to as the middle Rio Grande. Platania (1993) first documented the rapid decline

of the species in the middle Rio Grande in the late 1980s. Since 1993, systematic demographic monitoring has been conducted from April to October at 20 localities encompassing the species current range, revealing recurrent order-of-magnitude declines in the population (e.g., Dudley et al. 2019). Population declines are typically associated with periods of reduced spring runoff and prolonged periods of low flow over the summer months (Archdeacon 2016; Dudley et al. 2019; Figure 1). Conversely, periods of elevated and protracted spring flows and limited summer drying are associated with increased abundance. Periods of greatly reduced densities (<1 fish per 100 m^2) were documented between 2000-2004, 2006, 2012-2015 and in 2018 (Dudley et al. 2019) while 1996, 2010 and 2011 were only marginally better (1-2 fish per 100 m^2). Highest densities were recorded in 1995, 2005 and 2017 (estimated densities 23.17 – 44.85 fish per 100 m^2). These data confirm that declines can be precipitous from one year to the next, and that the species has the capacity to recover following periods of low abundance. Large-scale propagation began in 2002-2003 with annual spring collections of hundreds of thousands of eggs from riverine spawning. Eggs were reared in captivity and released as pre-reproductive adults the following winter. Incorporation of eggs produced from riverine spawning into hatchery activities, captive spawning of wild-origin individuals, and annual augmentation are now cornerstones of recovery efforts for the species (U.S. FWS 2018a). Genetic monitoring began in 1999 and is conducted annually using microsatellites and mitochondrial DNA markers (Osborne et al. 2012). Metrics tracked include standard diversity measures (Nei's unbiased gene diversity [uH_S], observed heterozygosity [H_O] and allelic richness [A_R]), the variance genetically effective population size (N_{eV}), and the linkage disequilibrium effective population size (N_{eD}).

To allow genetic data to be interpreted with reference to population demography, the number of wild-born and augmented fish in each year were estimated using a population model

179 (Yackulic et al., In Press). The model integrates Rio Grande silvery minnow abundance estimates
180 made from 2008-2011 (Dudley et al. 2012), with catch-per-unit-effort (CPUE) data collected
181 monthly between April and November, along with estimates of habitat availability. Abundances
182 were directly estimated by the model for each year between 2002 – 2018. Abundances for 1999
183 and 2000 were extrapolated by analyzing observed river discharge and catch-per-unit-effort data
184 in a Bayesian model that used parameter estimates and associated uncertainty to estimate prior
185 distributions.
186
187 *Sample selection*
188 Samples for SNP identification were selected from archived Rio Grande silvery minnow held at
189 the Museum of Southwestern Biology, Division of Fishes. Samples were selected based on: (1)
190 preservation method (frozen or 95% ethanol); (2) year of collection (the earliest ethanol/frozen
191 material was collected in 1999); and (3) collection locality (Table S1). We selected samples that
192 represented the temporal scale of ongoing genetic monitoring (1999-2018) and bracketed
193 population bottlenecks identified from demographic monitoring (Figure 1). We included ~10
194 samples from each of three populated river reaches (Angostura, Isleta and San Acacia - when
195 available) to reflect the spatial scale of monitoring, which encompasses the entire geographic
196 range of the species. Population genetic analysis was based on total number of samples (pooled
197 across reaches), since there is little evidence of population structure between reaches (Osborne et
198 al. 2012). Additional samples were included from 1999 and 2000 to provide redundancy in the
199 event of poor sample quality (i.e., degraded DNA) in older samples, and to obtain genomic data
200 prior to the beginning of the conservation hatchery and augmentation program. To ensure
201 representative coverage of the time series (i.e., a sample every 2 years) we purified archived

DNA (originally isolated using a proteinase-K and phenol-chloroform protocol) when tissue samples were not available (Table 1). A total of 379 samples were included for DNA sequencing. Sequence quality was assessed by preservation type using the non-parametric Kruskal-Wallis test implemented in the R package *stats* v. 4.0.3 (details in Figure S1).

NextRAD Sequencing

Isolation of DNA from tissue samples was performed using E.Z.N.A.® tissue DNA (Omega Bio-Tek Inc, Norcross, GA, USA) or Zymo™ Quick-DNA (Zymo Research Corp, Irvine, CA, USA) kits according to the procedures outlined by the manufacturer. Isolations of DNA from previous genetic monitoring were purified using Zymo™ DNA clean and concentrator® kits to remove phenol which can inhibit DNA sequencing. All samples were treated with RNase A. Each isolate was evaluated for the presence of high molecular weight DNA and the absence of RNA contamination by electrophoresis on a 1.2 % agarose gel. Double-stranded DNA was quantified using Qubit BR assays (Invitrogen, Thermo Fisher Scientific) and samples with sufficient high-quality DNA were submitted for sequencing at SNPsaurus, LLC (University of Oregon, OR, USA). Genomic DNA was converted into Nextera-tagmented reductively-amplified DNA genotyping-by-sequencing (nextRAD) libraries and sequenced according to Russello et al. (2015). Additional details are provided in the supplementary material. Genomic DNA fragments were pooled in two nextRAD libraries, each sequenced on two Illumina® Hi-Seq 4000 lanes of 150 base pair (bp) single-end reads.

Microsatellites

Microsatellite data from nine loci previously genotyped in samples spanning the period 1999 – 2010 (Osborne et al. 2012; supplementary material) were used in this study for comparative analysis. In addition, microsatellite data was included from 1,570 individuals collected as part of ongoing monitoring for 2012, 2015, 2017, and 2018 from the Rio Grande using methods described previously. These data from these additional years were paired directly with microhaplotype data.

Variant calling and quality filtering

Raw DNA sequences obtained from nextRAD sequencing from 379 individuals were demultiplexed by sequencing lane and unique DNA barcode combinations that identified individuals. Raw reads were trimmed and aligned to a draft female Rio Grande silvery minnow reference genome. Resulting nextRAD loci were used to call variants that were subsequently filtered to obtain a biallelic SNP dataset. Next, the variable positions in each locus were haplotyped (hereafter referred to as microhaplotypes) using the dDocent pipeline (Willis et al. 2017). Finally, we tested microhaplotypes for deviations from Hardy-Weinberg equilibrium (HWE) and in linkage disequilibrium (LD). A detailed description of the procedure, software, filters and options employed to obtain the final dataset is presented in Table S2.

Genetic diversity

We calculated the percentage of missing data (% MD) per individual and locus for both datasets using program GenoDive (Meirmans 2020). Large % MD affects estimation of some metrics (e.g., F_{IS} and N_e), adding uncertainty that confounds interpretation of downstream results (e.g., Marandel et al. 2020). We calculated standard genetic diversity metrics typically used in genetic

monitoring programs, including Nei's unbiased gene diversity (Nei 1987) and heterozygosity for each temporal sample using the program GenoDive v. 3.0 (Meirmans 2020) to enable comparisons between marker types. Allelic richness and average inbreeding coefficients (F_{IS}) were calculated using the R package *diveRsity* v. 1.9.90 (Keenan et al. 2013). The 95% confidence intervals (CIs) were calculated for uH_S, H_O and F_{IS}. For microsatellites, GENEPOP'007 (Rousett 2008) was used to test for departures from Hardy-Weinberg equilibrium (HWE) using the procedure of Guo and Thompson (1992) and to perform global tests for linkage disequilibrium for all pairs of loci in each collection. Sequential Bonferroni correction (Rice 1989) was applied to account for inflated Type I error rates associated with multiple simultaneous tests. We used Pearson correlations to examine whether % MD was correlated with diversity metrics and to evaluate concordance between comparable metrics estimated from microsatellites and microhaplotypes.

Genetic effective population size

The linkage disequilibrium method (Hill 1981) was used to estimate the N_{eD} for each collection of Rio Grande silvery minnow as implemented in the NeEstimator v. 2.0 software package (Do et al. 2014). Low frequency alleles ($P_{crit} = 0.02$) were excluded from the microsatellite dataset singleton alleles were removed for microhaplotypes prior to analysis. Estimates of N_{eD} are an approximation of the effective number of parents that produced the year class from which the sample was taken (Waples 2005). For microhaplotypes 95% CIs for N_{eD} were calculated using a jackknife approach recommended for datasets with large numbers of loci (Jones et al. 2016) because parametric confidence intervals are too narrow when locus pairs are not entirely independent (Gilbert and Whitlock 2015). For consistency, we also used the jackknife method to

generate CIs for microsatellites, but these did not differ greatly from parametric CIs. Three estimates of $N_{eD} = \infty$ were obtained across the two datasets (1999, 2000- microsatellites; 2000-microhaplotypes; see *Results* section). Infinite estimates occur when results can be explained entirely by sampling error, and is usually interpreted as a large value of N_{eD} (Waples and Do 2010). We used the equation

$$N_{e(inf)} = N_{e(max)} + SD_{Ne}$$

to adjust estimates for subsequent analysis, where $N_{e(inf)}$ is the value used to replace infinite estimates, $N_{e(max)}$ is the largest N_e estimate obtained, and SD_{Ne} is the standard deviation calculated across all N_e estimates by marker type (Gossieaux et al. 2019).

Variance effective population size (N_{eV}) was calculated using the temporal method (Nei and Tajima 1981). Confidence intervals for N_{eV} were obtained using the parametric approach (Waples 1989). We used a P_{crit}=0.02 to exclude low frequency alleles (Waples and Do 2010) to reduce biased estimates of N_e associated with rare alleles (Hedrick 1999; Turner et al. 2001). To account for small deviations from the discrete generation model, we corrected consecutive estimates (i.e., 1999-2000, 2008-2009, 2009-2010, 2017-2018) of N_{eV} for overlapping generations as described previously (Turner et al. 2006; Osborne et al. 2012). We used Rosner's Test (Rosner 1983) to detect outliers in N_{eV} and N_{eD} estimates. Four outlier N_{eD} values (1999, 2000, 2010, 2012) were detected in the microsatellites data. Consequently, a Spearman correlation was used to examine the relationship between N_{eD} estimates obtained with microsatellites and microhaplotypes. Single outlier N_{eV} values were detected in the microsatellite and microhaplotype dataset; 2015-2017 and 2002-2004 respectively. Relationships

between N_{eV} obtained with microsatellites and microhaplotypes were evaluated using Pearson correlation as the outliers did not affect this analysis. These analyses were performed in R using the *ggpubr* package v. 0.4.0.999 (Kassambra 2020).

Temporal differentiation

Temporal genetic structure was evaluated using *k*-means clustering to estimate the optimal number of population groups in our datasets and using discriminant analysis of principle components (DAPC). DAPC summarizes genotypes in principle components which are used to construct linear functions that maximize among group variation while minimizing within group variation. Both analyses were performed using the R package *adegenet* v. 1.3-1 (Jombart and Ahmed 2011). *K*-means clustering was used for *de novo* group identification, where *k* is the number of groups, using both datasets. A group was defined as a distinct genetic sample taken at a particular time. Bayesian Information Criteria (BIC) were used to select *k* with the lowest BIC value. Prior to DAPC we replaced missing data within each group using the Breiman's regression random forest algorithm (Breiman 2001) implemented in R package randomForest v. 4.6–14 (Liaw and Wiener 2002). Values of missing data in the microhaplotype (3% total MD) and microsatellite (2% total MD) datasets were predicted from 500 independently constructed regression trees and 50 bootstrap iterations with default bootstrap sample size. This was preferred over the default "mean method" (i.e., missing genotypes are replaced by the average estimated across the dataset) implemented in *adegenet*, to ensure that we did not artificially increase similarity of allele frequencies across years. For each marker type, a first DAPC was performed using years as groups, without scaling allele frequencies, retaining all PCA and DA axes, and keeping other options as default. The *a-score* method was used with the results of the

316 first DAPC to select the optimal number of principle components retained for the final DAPC,
317 while keeping the other options as in the first DAPC. Levels of diversity (number of alleles and
318 heterozygosity) differ between microsatellites and microhaplotypes (dominated by biallelic
319 SNPs), hence we calculated pairwise values of G''_{ST} (Meirmans and Hedrick 2011) and 95% CIs
320 between temporal samples using *diveRsity* for both datasets. Confidence intervals were
321 calculated using 999 bootstrap replicates. We used a Mantel test implemented in R (*mantel.rtest*)
322 with 9999 replicates to compare the values of G''_{ST} obtained for microsatellite and
323 microhaplotypes. All analyses were conducted in R studio v. 1.3.1093-1 using R v. 4.0.3 (R Core
324 Team 2020).
325
326 *Evaluation of inbreeding metrics for genetic monitoring*
327 In addition to 'standard, genetic diversity metrics (Osborne et al. 2012), we added metrics of
328 inbreeding to the genetic monitoring time-series. We calculated standardized multilocus
329 heterozygosity (sMLH) for individuals in each temporal sample based on microsatellite and
330 microhaplotype loci using the package *inbreedR* (Stoffel 2016) implemented in R. Measures of
331 inbreeding, including internal relatedness (IR) and mean identity by descent (IBD) inbreeding
332 co-efficient ($\bar{F}$) were calculated using the programs GENHET (Coulon 2010) and EMIBD9 vers
333 1.0 (Wang 2021), respectively. We used Pearson correlations and biplots to visualize
334 relationships of $\bar{F}$ and sMLH/IR for both datasets.
335
336 We measured identity disequilibrium using the $\hat{g}_2$ statistic for each temporal sample (Szulkin et
337 al. 2010; David et al. 2007). To test whether $\hat{g}_2$ was significantly different from zero, genetic
338 data were permutated 1000 times to generate a *p*-value for the null hypothesis of no variance in

inbreeding (i.e., $\hat{g}_2$=0; David et al. 2007; Stoffel et al. 2016). Bootstrap replicates (n = 1000) were used to generate 95% CIs. We used the non-parametric WAVK test (Wang et al. 2008) (with moving window = 3) using the R package *funtimes* vers. 8.2 (Lyubchich and Gel 2022) to examine if there were any significant trends (monotonic or non-monotonic) for values of $\bar{F}_{pop}$, $\hat{g}_2$ or F_{IS} over the time series. Values were considered significant when $p < 0.05$. In cases where a significant trend was detected, we used a Mann-Kendall test (MK; Mann 1945) to determine if the trend was monotonic (reported as Kendall's τ) using the R package *trend* (Pohlert 2020). The magnitude of the change was calculated using Sen's slope (Sen 1968) at the 5% significance level. The Standard Normal Homogeneity Test (SNHT) implemented in *trend* was used with one million Monte-Carlo replicates to identify transitions (i.e., change-points) when a significant trend was detected (microhaplotype-based $\bar{F}$, $\hat{g}_2$).

Results

Quality of samples based on preservation method and year of collection

The median number of mapped reads did not differ significantly between DNA isolated from frozen tissue and purified DNA from archived phenol-chloroform-extracted isolates (Figure S1). Median number of reads was higher for DNA from frozen tissue samples compared to ethanol-preserved material. There were also differences among temporal collections, but the number of mapped reads was relatively high in all cases (3.1 – 3.4 M reads per individual for all preservation methods).

Variant calling and quality filtering

After sequencing the nextRAD libraries and demultiplexing the raw sequences, an average 3.4 million (M) sequences per individual (minimum=1.1 M; maximum=5.5 M) were obtained. After alignment to a draft reference genome, an average of 1.27 M reads per individual were retained for further SNP search (minimum=0.9 M; maximum=5.3 M). The total number of reads, variants, and individuals retained after each step of the bioinformatics pipeline are shown in Table S2.

Summary of genetic monitoring data for Rio Grande silvery minnow

The final dataset consisted of 3,151 loci comprising 5,549 SNPs from 366 individuals. Loci that were multiallelic (2-12 alleles per locus) comprised 42.5% of loci. The remainder (57.5%) were single biallelic SNPs. Although we collectively refer to this dataset as microhaplotypes, we acknowledge that most loci characterize variation at single sites. Across all years, a total of 8458 microhaplotype alleles were observed compared to microsatellites 240 alleles. Across both datasets (microsatellite and microhaplotypes) we did not observe correlations between the percentage of missing data and diversity metrics (Table S3) with the exception of microhaplotype-based allelic richness (r=-0.71, p=0.011). Likewise, % MD was not correlated with either $\hat{g}_2$ or $\bar{F}_{pop}$ for either dataset. Out of 37,932 total HWE tests (3,161 loci across 12 years) based on microhaplotypes, 9.1% departed from HWE. No loci departed from HWE consistently across the time-series thus all loci were retained. Additionally, 10 loci were consistently found in LD and discarded, retaining 3,151 loci. Of 108 total HWE tests (9 loci across 12 years) based on microsatellite data, departures from HWE were detected in 37% of the tests. Across years, LD was detected between three pairs of microsatellite loci (*Lco6* and *Lco*7; *Lco*1 and *Ca*6; *Lco*3 and *Ca*8). We retained all loci as we have previously shown that this

strategy does not affect downstream analyses (Turner et al. 2006). Microsatellite-based H_O was lower in 1999-2002 and 2009-2010 compared to other years (Figure 2, Table S4). However, overlapping CIs for all microsatellite estimates of H_O and uH_S indicated no difference across time.

Two N_{eD} estimates based on microsatellites (2004 and 2015) and microhaplotypes (2006 and 2015) were smaller than other temporal samples (Figure 3). Conversely, infinite N_{eD} estimates were observed in 1999 for both data sets, and likely resulted from small sample size rather than a true large effective population size. Otherwise, for both datasets, temporal estimates of variance effective population size, N_{eV}, were uniformly about one order of magnitude smaller than estimates of N_{eD} and ranged from 33 (1999-2000) to 604 (2015-2017) for microsatellites and from 122 (2008-2009) to 576 (2002-2004) for microhaplotypes (Table S4).

DAPC based on *k*-means clustering of microhaplotype and microsatellites data indicated the best solution as $k = 1$ (Figure 4). In the DAPC plot based on microsatellites, the 2015, 2017 and 2018 ellipses were shifted to the right on the first discriminant axis indicating a shift in allele frequencies. Microhaplotype-based DAPC exhibits the same qualitative pattern. Values of pairwise G''_{ST} ranged from 0.003 to 0.095 for microsatellites and from 0.002 – 0.008 for microhaplotypes (Figure S2).

Comparisons between microsatellites and microhaplotypes

Gene diversity and H_O obtained from microsatellites were not significantly correlated with those obtained from microhaplotypes (Table 3). Allelic richness was negatively correlated between datasets ($r_{(df=11)} = -0.70$, $p = 0.012$) however, the actual difference in microhaplotype-based values of A_R between temporal samples was negligible. Confidence intervals were wider for

407 microsatellites compared with microhaplotypes for all diversity metrics (Figure 2). Estimates of
408 N_{eD}, were similar in magnitude between markers and had overlapping confidence intervals
409 across the time series (Table S4, Figure 3). Estimates of N_{eD} from microhaplotypes were
410 significantly correlated with estimates based on microsatellites ($r_{s(df=11)} = 0.647$, $p = 0.023$).
411 Microhaplotype-based estimates of N_{eV} were not strongly associated with estimates derived from
412 microsatellites ($r_{(df=9)} = 0.136$, $p = 0.689$). Mantel correlations between pairwise values of G''_{ST}
413 obtained using these two datasets were significantly positively associated. Microhaplotype-based
414 estimates of G''_{ST} were small between temporal samples and not different from zero (Figure S2)
415 while microsatellite-based values were significantly different from zero except for comparisons
416 between the most recent temporal collections (2015-2017, 2015-2018).
417
418 *Evaluation of inbreeding metrics for genetic monitoring*
419 When compared with microhaplotypes, sMLH and IR based on microsatellites had a wider range
420 of values within years, but mean values varied little across the time series (Figure 5).
421 Microhaplotype-based values of IR had a narrower range such that an increase in IR could be
422 detected for the period 2009-2017 compared to other years (1999-2016, 2018). This same pattern
423 was not evident from the microhaplotype-based sMLH values. Values of $\bar{F}_{pop}$ calculated from
424 microsatellites varied from 0.13 (2015) to 0.27 (2002) while $\bar{F}_{pop}$ values based on
425 microhaplotypes were smaller ranging from 0.02 (2017) to 0.14 (2018). At the individual level,
426 there was a strong correlation between microsatellite-based sMLH ($r_{(df=11)} = -0.95$, $p < 0.00001$)
427 and IBD $\bar{F}$ for microsatellites. This result was mirrored for microhaplotype-based sMLH (r
428 $r_{(df=11)} = -0.76$, $p < 0.001$; Figure 6). IR was also strongly correlated and IBD $\bar{F}$ regardless of

marker type. For both sMLH and IR, the correlation with $\overline{F}$ was stronger for microsatellites compared to microhaplotypes.

No trend was identified by microsatellite-based estimates of $\overline{F}$, $\hat{g}_2$ or F_{IS} or for microhaplotyped-based F_{IS} across the time series (Table S5, Figure 7). Monotonic trends were detected for microhaplotype-based estimates of $\overline{F}_{pop}$ ($\tau = 0.485$; $p = 0.017$; slope = 0.006, p 0.034; Figure 7, Figure 8) and $\hat{g}_2$ ($\tau = 0.697$; $p = 0.001$; slope = 0.001, $p = 0.002$) which increased across the time series. Microhaplotype-based estimates of F_{IS} and $\overline{F}_{pop}$ had narrower CIs compared to those derived from microsatellites while some of the CIs for $\hat{g}_2$ were wider for microhaplotype-based estimates but these did not overlap with zero.

Discussion

Summary of genetic monitoring data for Rio Grande silvery minnow- insights from microhaplotypes

Two decades of microsatellite-based genetic monitoring in Rio Grande silvery minnow has provided information critical to ongoing adaptive management (Table 5). Conclusions from microhaplotype data largely agree with interpretations based on microsatellites but inclusion of additional metrics provide additional insight into the complex dynamics in this population. Microhaplotype-based estimates of diversity reinforces that genetic variation has been maintained despite periodic population collapse. This resilience is attributable to ongoing population augmentation and integrated management of wild and captive populations (Osborne et al. 2012, 2020). More precise population and individual diversity estimates (uH_S, H_O, IR) based on microhaplotypes revealed patterns of genetic change over time not detected by microsatellites; highlighting one of the benefits of transitioning to microhaplotype-based

genomic monitoring. Additionally, microhaplotypes were more sensitive to shifts in temporal genetic diversity where DAPC clearly indicated a distinct allele frequency shift. Larger shifts corresponded to periods of extremely low wild abundance when heavy population augmentation was employed to replenish the wild spawning stock resulting in genetic drift. A persistent allele frequency shift after 2014 marks the replacement of the wild population with stocks derived from relatively few captive breeders (i.e., slightly different allele frequencies compared to the pre-bottleneck population).

Microhaplotype-based estimates of contemporary genetic effective size were also consistent with microsatellites in showing that N_{eV} is small (< 250) for most pairwise comparisons, and values of N_{eV} are consistently smaller than N_{eD}. Estimates of N_{eV} generally had tight confidence intervals regardless of data types, confirming that alternative sampling strategies that use (i) more individuals but fewer loci (microsatellites) or (ii) fewer individuals but more loci have similar power to estimate this metric (e.g., Waples 1989). Consistency of results obtained from microhaplotypes with previous microsatellite data is important as contemporary N_e is a critical determinant of diversity loss from the population. The smallest values of N_{eD} (both data types) were seen in samples collected immediately following population bottlenecks (2004, 2006, 2015). These findings are consistent with Antao et al. (2010) who found that N_{eD} reliably detected less severe population declines a few generations after the event.

The underlying causes for differences between N_{eV} and N_{eD} have been explored previously. Briefly, Carson et al. (2020) used simulations to show that N_{eD} and N_{eV} respond differently to augmentation and dispersal/ fragmentation. Specifically, N_{eD} measured in the wild population reflects the global effective size of the total population (wild + hatchery) and hence at higher augmentation rates N_{eD} should be larger. In contrast, augmentation has the opposite effect

on N_{eV} because augmentation acts as an additional source of 'genetic drift' such that N_{eV} is reduced with heavier augmentation. In reality, N_{eV} and N_{eD} estimated for the Rio Grande silvery minnow population do not always respond as predicted because simulations cannot capture all complex interactions between demography of the wild population that experiences large swings in population size from year to year, with simultaneous management actions.

Genomic signatures of population bottlenecks and augmentation were also revealed by considering measures of inbreeding not traditionally used in genetic monitoring programs. Trends in $\hat{g}_2$ and $\bar{F}$ calculated from microhaplotypes suggested that incorporating these metrics into genetic monitoring programs would be a valuable addition and could enable study of relationships of GWH to fitness in a managed population. Further investigation is necessary to fully understand how these metrics respond to complex demographic scenarios. Microsatellites appeared to be less sensitive to these temporal trends; likely because of the small number of loci compared to microhaplotypes.

Comparisons between microsatellites and microhaplotypes

Comparisons of microsatellites and microhaplotypes allowed us to evaluate the relative consistency, precision, and sensitivity to missing data between marker types (Table 4). Off all the metrics we evaluated, we found that only microhaplotype-based estimates of A_R were sensitive to the low levels of missing data in our study. Even with relatively small sample sizes, microhaplotypes yielded more precise estimates of diversity (uH_S, H_O, IR) and N_{eV} compared to microsatellites, allowing temporal changes to be detected in the time-series. On the other hand, microhaplotye-based A_R was not an informative metric. Like other studies (*e.g.*, Zimmerman et al. 2020; Fischer et al. 2017; Lemopoulos et al. 2019) and important for ongoing monitoring

498 efforts in Rio Grande silvery minnow, we found that measures of divergence (G''_{ST}) were
499 positively correlated between markers and this was also true of N_{eD}. Hence, when these metrics
500 (G''_{ST} and N_{eD}) are measured with only SNP-based markers in the near future, we can be
501 relatively confident that signals of divergence or changes in effective population size accurate
502 rather than a consequence of change in marker type. Although CIs were often large for N_{eD}
503 regardless of data type, trends in annual point estimates makes N_{eD} a particularly important
504 metric for adaptive species management when interpreted in the context of population
505 demography.
506 Weak correlation of diversity metrics between datasets suggests that diversity estimated
507 from a small number of microsatellites may not sufficiently reflect genomic diversity
508 (Lemopoulos et al. 2019; Guillot and Foll 2009). Other studies failed to find significant
509 correlations between some diversity metrics estimated from microsatellites and SNPs (e.g.,
510 Fischer et al. 2017; Zimmerman et al. 2020; DeFaveri et al. 2013). Charkraborty (1981) and
511 DeFaveri et al. (2013) concluded that variation in heterozygosity across the genome would result
512 in lack of correlation of diversity measures when estimates from a small number (<20) of
513 molecular markers; such as in our study. Lack of correlation between markers sets for uH_S and
514 H_O may also be caused by (i) ascertainment bias, (ii) typing artefacts (microsatellites), (iii)
515 underlying evolutionary processes affecting per locus levels of diversity, and (iv) genomic
516 location of the markers (e.g., DeFaveri et al. 2013).
517 Microsatellites are typically found in non-coding regions of the genome such as introns
518 and intergenic regions, evolve primarily by replication slippage, and thus have high mutation
519 rates (Ellegren 2004). Loci are typically selected for population genetic studies based on levels
520 of diversity such that more polymorphic loci (higher number of alleles and heterozygosity) are

preferred, yielding greater sensitivity to changes in population size and genetic diversity. Reductions in microsatellite allelic diversity were detected in Rio Grande silvery minnow from 1999 to 2000 (before population augmentation began) and in 2012 and 2015 that bracketed order of magnitude declines in the middle Rio Grande population. Substantial declines in allelic diversity were not seen in the rest of the time series (except in 2017), a result that we attribute to repeated population augmentation (Osborne et al. 2012). Declines in A_R were not detected with microhaplotypes because of reduced sensitivity because loci are dominated by biallelic SNPs. Our results suggest that SNPs obtained from high throughput NGS protocols could be more important to monitor as they represent a broader picture of genomic variation as many more loci as assayed; including coding and non-coding regions.

Low allelic variability at individual microhaplotype loci is offset by a substantially higher number of loci such that the larger number of total number of alleles assayed yielded more precise estimates of diversity (i.e., smaller confidence intervals) when compared with microsatellites in Rio Grande silvery minnow. For example, microhaplotype-based heterozygosity was higher in 2018 (and IR was lower) compared to previous years reflected by a negative inbreeding coefficient while F_{IS} and IR increased between 2009-2017 compared to values observed from 1999-2008. These changes are indicative of departures from Hardy-Weinberg proportions. An excess of heterozygotes in 2018 and deficit in 2009-2017 is likely a 'Wahlund' or sampling effect (Waples 2015) that occurred when fish from the middle Rio Grande population and different hatchery sources were mixed by augmentation. Different proportions of wild to captive fish may also affect the value of F_{IS} because the magnitude of the Wahlund effect increases with population divergence in allele frequencies and the evenness of mixture proportions (Waples 2015).

Evaluation of inbreeding metrics for genetic monitoring

In Rio Grande silvery minnow, we found that sMLH and IR were strongly associated with $\bar{F}$ and F_{IS} for both datasets. The strength of observed correlations between individual $\bar{F}$ and sMLH and IR in Rio Grande silvery minnow was greater than in other species including zebra finch (range $r^2 = 0.46 - 0.49$; Forstmeier et al. 2012) but within the range seen in oldfield mice ($r^2 = 0.74$; Hoffman et al. 2014). Strong correlations were also reported between genomic measure of inbreeding based on runs of homozygosity (F_{ROH}) and heterozygosity (MLH) in wolves ($r^2 = 0.91$; Kardos et al. 2018). The genomic measures of inbreeding used here (e.g., MLH, IR, $\hat{g}_2$) characterize variation in inbreeding due to all IBD segments of the genome including those arising from both recent and distant ancestors (Keller et al. 2011; Kardos et al. 2018). These metrics may be more accurate than alternative pedigree-based estimates that make the unrealistic assumption of unrelated ancestors. In cases where there is high variance in $\bar{F}$ (e.g., 2018), genomic measures of individual inbreeding (e.g., IR and sMLH) are expected to be more precise (Miller et al. 2014; Kardos et al. 2018; Kardos et al. 2014); consistent with microhaplotype data.

Variance in inbreeding in some years (Figure 8) was also reflected in microhaplotype-based values of $\hat{g}_2$ that were significantly different from zero. In contrast, microsatellite-based $\hat{g}_2$ values were not informative about underlying identity by descent because in the majority of cases, $\hat{g}_2$ did not differ from zero. Other authors (e.g., Hoffman et al. 2014; McLennan et al. 2019) also found that compared with microsatellites, $\hat{g}_2$ estimated from large numbers of SNP-based markers provided a more accurate measure of inbreeding and GWH because of increased statistical power associated with the number of SNP loci screened. Likewise, Kardos et al.

(2014) found that when estimated from few microsatellite loci $\hat{g}_2$, was not significant even in cases when heterozygosity fitness correlations were present.

Identity disequilibrium ($\hat{g}_2$) can occur when genetic drift/bottlenecks yield a higher incidence of consanguineous matings as a consequence of small population size. Moreover, populations that have experienced multiple bottlenecks may have inflated inbreeding values (Robinson et al. 2013). Miller et al. (2014) found that ID was substantially higher ($\hat{g}_2$ = 0.06) in a population of bighorn sheep that had experienced a population bottleneck and was subsequently "rescued" by introduction of individuals from a neighboring population, when compared to a native population ($\hat{g}_2$ = 0.004). Values of $\hat{g}_2$ observed in Rio Grande silvery minnow at several time-points ($\hat{g}_2$ = 0.01-0.019 in 2008, 2017-2018) are considered high for a natural population (Hoffman et al. 2014). For example, most microhaplotype-based values of $\hat{g}_2$ in Rio Grande silvery minnow were larger than in a small red deer population (*Cervus elaphus*; $\hat{g}_2$ = 0.001; Huisman et al. 2016) and in a large population in storm petrel (*Oceanodroma leucorhoa;* $\hat{g}_2$ = 0.001; Sin et al. 2021). Like Rio Grande silvery minnow, the population of deer has experienced bottlenecks and admixture between different populations (Huisman et al. 2016). Sin et al. (2021) noted that in storm petrel, mating system and inbreeding between close relatives could not account for variance in inbreeding, and hence, suggested that observed variance in inbreeding was explained by past population bottlenecks along with more recent declines in N_e and low levels of admixture between Atlantic and Pacific populations of petrels. Footprints of bottlenecks persist even after the population has recovered (Bierne et al. 2000) and can still cause inbreeding depression (Sin et al. 2021).

Values of microhaplotype-based inbreeding metrics were notably higher for the majority of recent time points from 2008- 2018 compared to earlier periods (1999 to 2006). Early

589 augmentation efforts (2002-2007) of the wild population of Rio Grande silvery minnow were
590 comprised largely of stocks reared from wild-caught eggs (WCE) rather than offspring of captive
591 spawning. Stocks reared from WCE typically have allele frequencies nearly identical to the wild
592 population (Osborne et al. 2012). After that time, released fish were increasingly derived from
593 captive spawning and hence derived from fewer parents than wild-produced stocks. Some
594 increases in microhaplotype-based values of $\bar{F}_{\text{pop}}$ and $\hat{g}_2$ follow periods of heavy population
595 augmentation (Figure 1). For example, the estimated breeding population in the spring of 2007
596 was comprised of roughly equal numbers of wild and augmented fish while from 2013-2015 the
597 number of augmented fish far exceeded the number of "wild-born" individuals as efforts were
598 made to rebuild the population following its collapse during the drought from 2012-2014
599 (Yackulic et al. In Press). Drought years represent periods when genetic drift is expected to be
600 high because (i) the bottleneck reduces the number of breeders, (ii) captive spawning involves
601 only a subset of the population, and (iii) only a subset of hatchery fish persist after release. Rio
602 Grande silvery minnow exhibits type-III survivorship such that females are highly fecund
603 (Caldwell et al. 2019) but in the wild there is very high mortality of early life stages such that a
604 small proportion of the offspring survive to recruit to the riverine adult population (Horwitz et al.
605 2018). In contrast, use of captive spawning reduces variance in reproductive success among
606 captive spawners and their offspring are eventually released to the river. In the following year,
607 there may be breeding between slightly related individuals (reflected by larger values of F) as
608 well as breeding between relatively unrelated individuals (e.g., wild with augmented fish, and
609 smaller values of F); resulting in greater variance in population F and reflected by significant
610 values of $\hat{g}_2$ (e.g., 2018). Admixture between populations with different allele frequencies causes
611 gametic associations (i.e., LD) between loci as a function of the difference between the parental

612 populations and the admixture rate (Chakraborty and Weiss 1988) and the effects of admixture
613 can be variable and can either increase or decrease GWH depending on the magnitude of
614 admixture and the genetic background of the population (Vendrami et al. 2020). Importantly, in
615 both red deer and storm petrel where variance in inbreeding was less than seen recently in Rio
616 Grande silvery minnow, general effects HFC were observed implying inbreeding depression in
617 both a small (Keller et al. 2016) and a large population (Sin et al. 2021). Hence, inclusion of
618 inbreeding metrics in genetic monitoring of both wild and captive populations of Rio Grande
619 silvery minnow can provide valuable information for adaptive management of the species (e.g.,
620 altered augmentation strategies).

621 *Recommendations for genetic monitoring of Rio Grande silvery minnow*
622 For ongoing genetic monitoring in Rio Grande silvery minnow, a subset of the loci used in this
623 study will be incorporated into a Genotyping-in-Thousands by sequencing panel (GT-seq;
624 Campbell et al. 2015). This is a method of targeted SNP genotyping that uses multiplexed PCR
625 amplicon sequencing and allows consistent genotyping of hundreds of target SNPs across
626 hundreds to thousands of individuals. For genetic monitoring programs, GT-seq is time and cost-
627 effective once multiplexed PCRs are optimized. (Campbell et al. 2015). Additionally, GT-seq
628 panels should allow consistent genotyping across laboratories; which can be troublesome with
629 microsatellites without considerable validation. Preliminary results show that 300 loci are
630 sufficient to represent patterns of population and individual diversity contained in the complete
631 dataset presented in this study (data not shown). Our results demonstrate that it is now possible
632 for conservation programs to incorporate genomic methods into routine monitoring.
633 Development of genomic tools for this species and others will allow (i) less expensive
634 monitoring, (ii) more rapid evaluation of captive stocks prior to release to the wild, (iii)

retrospective analysis of archived wild and captive material and (iv) will facilitate further evaluation of inbreeding metrics and selection.

More broadly, results presented herein highlight the importance of archiving both tissue and DNA samples collected during long-term monitoring so they can be utilized as new genomic technologies are developed. Despite differences in ages of genetic samples and differences in how samples were stored, sequencing depth was sufficient to estimate parameters of interest with generally greater precision than microsatellite data. Archiving biological material (preferably tissue) is important not only for imperiled species with on-going genetic monitoring programs, like Rio Grande silvery minnow, but also for species of conservation concern without established conservation programs; guaranteeing the availability of genetic material in the future. In the case of Rio Grande silvery minnow and many other imperiled species, sampling is often non-destructive so there may not be tissue samples remaining after DNA isolation and in these cases archiving DNA samples along with associated metadata is imperative. Our results are encouraging as they suggest that researchers have some flexibility in sample choice including DNA isolates when transitioning from one marker set to another.

Acknowledgements

We sincerely thank Alexander Cameron, David Camak, Samuel McKitrick for assistance in the field, laboratory, and with bioinformatics. We thank Emily DeArmon and Alexandra Snyder in the UNM Museum of Southwestern Biology Division of Fishes for expert curatorial services. Thomas Archdeacon (US Fish and Wildlife Services), Charles Yackulic (U.S. Geological Service) provided data, discussions, and insights that greatly improved the manuscript. Comments from four anonymous reviewers improved the manuscript. High performance

computing was conducted at the UNM Center for Advanced Research Computing that is supported, in part, by the National Science Foundation. We also thank Eric Gonzales and Jennifer Bachus (U.S. Bureau of Reclamation). This study was funded by the U.S. Bureau of Reclamation (R18AP00130). Samples were collected under permits from the New Mexico Department of Game and Fish (3015), U.S. Fish and Wildlife Service (TE38055-0), and a protocol approved by the UNM Institutional Animal Care and Use Committee (#21-201194-MC).

Conflict of Interest

The authors declare no conflicts of interest.

Data accessibility sharing

Individual genotype data from microsatellites and microhaplotypes will be made available on Dryad and Fastq files will be made available on GenBank

Benefit-sharing statement

Results of our research are shared with the broader scientific and management community (see above), and our study addresses a priority concern, specifically the conservation of Rio Grande silvery minnow. Benefits from this research accumulate from the sharing of our data and results on public databases as described above. Results are also shared with management agencies charged with conservation of the species.

Author Contribution

MJO was responsible for project conception, design and coordination, laboratory work, data analysis, manuscript writing and revision, and obtaining funding. GCD was responsible for bioinformatics, data analysis, and writing the manuscript. TFT was responsible for project conception, sample curation, manuscript writing and revision and obtaining funding.

References

Alò, D., & Turner, T. F. (2005). Effects of habitat fragmentation on effective population size in the endangered Rio Grande silvery minnow. *Conservation Biology*, *19*(4), 1138-1148. https://doi.org/10.1111/j.1523-1739.2005.00081.x

Antao, T., Pérez-Figueroa, A., & Luikart, G. (2010). Early detection of population declines: high power of genetic monitoring using effective population size estimators. *Evolutionary Applications*, *4*(1), 144–154. https://doi.org/10.1111/j.1752-4571.2010.00150.x

Archdeacon, T. P. (2016). Reduction in spring flow threatens Rio Grande Silvery Minnow: trends in abundance during river intermittency. *Transactions of the American Fisheries Society*, *145*(4), 754-765. https://doi.org/10.1080/00028487.2016.1159611

Archdeacon, T. P., Diver-Franssen, T. A., Bertrand, N. G., & Grant, J. D. (2020). Drought results in recruitment failure of Rio Grande silvery minnow (*Hybognathus amarus*), an imperiled, pelagic broadcast-spawning minnow. *Environmental Biology of Fishes*, *103*(9), 1033–1044. https://doi.org/10.1007/s10641-020-01003-5

Archdeacon, T. P., & Reale, J. K. (2020). No quarter: Lack of refuge during flow intermittency results in catastrophic mortality of an imperiled minnow. *Freshwater Biology*, *65*(12), 2108–2123. https://doi.org/10.1111/fwb.13607

Balloux, F., Amos, W., & Coulson, T. (2004). Does heterozygosity estimate inbreeding in real populations? *Molecular Ecology*, *13*(10), 3021–3031. https://doi.org/10.1111/j.1365-294x.2004.02318.x

Beatty, G. E., Reid, N., & Provan, J. (2014). Retrospective genetic monitoring of the threatened Yellow marsh saxifrage (*S. axifraga hirculus*) reveals genetic erosion but provides valuable insights for conservation strategies. *Diversity and distributions*, *20*(5), 529-537.

Bennett, J. H., & Binet, F. E. (1956). Association between Mendelian factors with mixed selfing and random mating. *Heredity*, *10*(1), 51-55. https://doi.org/10.1038/hdy.1956.3

Bestgen, K. R., & Platania, S. P. (1991). Status and conservation of the Rio Grande silvery minnow, Hybognathus amarus. *The Southwestern Naturalist*, *36*(2), 225–232. https://doi.org/10.2307/3671925

Bierne, N., Tsitrone, A., & David, P. (2000). An Inbreeding Model of Associative Overdominance During a Population Bottleneck. *Genetics*, *155*(4), 1981–1990. https://doi.org/10.1093/genetics/155.4.1981

Breiman, L. (2001). Random forests. *Machine Learning*, *45*(1), 5-32.

Caldwell, C. A., Falco, H., Knight, W., Ulibarri, M., & Gould, W. R. (2019). Reproductive potential of captive Rio Grande silvery minnow. *North American Journal of Aquaculture*, *81*(1), 47-54.

Camak, D. T., Osborne, M. J., & Turner, T. F. (2021). Population genomics and conservation of Gila Trout (*Oncorhynchus gilae*). *Conservation Genetics*, *22*(5), 729-743. https://doi.org/10.1007/s10592-021-01355-0

Campbell, N. R., Harmon, S. A., & Narum, S. R. (2015). Genotyping-in-thousands by sequencing (GT-seq): a cost-effective SNP genotyping method based on custom amplicon sequencing. *Molecular Ecology Resources*, 15(4), 855-867.

Carson, E. W., Osborne, M. J., & Turner, T. F. (2020). Relationship of effective size to hatchery supplementation and habitat connectivity in a simulated population of Rio Grande silvery minnow. *North American Journal of Fisheries Management*, *40*(4), 922–938. https://doi.org/10.1002/nafm.10453

Chakraborty, R. (1981). The distribution of the number of heterozygous Loci in an individual in natural populations. *Genetics*, *98*(2), 461–466. https://doi.org/10.1093/genetics/98.2.461

Chakraborty, R., & Weiss, K. M. (1988). Admixture as a tool for finding linked genes and detecting that difference from allelic association between loci. *Proceedings of the National Academy of Sciences*, *85*(23), 9119–9123. https://doi.org/10.1073/pnas.85.23.9119

Coltman, D. W., Pilkington, J. G., Smith, J. A., & Pemberton, J. M. (1999). Parasite-mediated selection against inbred Soay sheep in a free-living, island population. *Evolution*, *53*(4), 1259. https://doi.org/10.2307/2640828

Coulon, A. (2010). GENHET: an easy-to-use R function to estimate individual heterozygosity. *Molecular Ecology Resources*, *10*(1), 167-169. https://doi.org/10.1111/j.1755-0998.2009.02731.x

David, P., Pujol, B., Viard, F., Castella, V., & Goudet, J. (2007). Reliable selfing rate estimates from imperfect population genetic data. *Molecular Ecology*, *16*(12), 2474–2487. https://doi.org/10.1111/j.1365-294x.2007.03330.x

DeWoody, Y. D., & DeWoody, J. A. (2005). On the estimation of genome-wide heterozygosity using molecular markers. *Journal of Heredity*, 96(2), 85-88. https://doi.org/10.1093/jhered/esi017

DeFaveri, J., Viitaniemi, H., Leder, E., & Merilä, J. (2013). Characterizing genic and nongenic molecular markers: comparison of microsatellites and SNPs. *Molecular Ecology Resources*, 13(3), 377–392. https://doi.org/10.1111/1755-0998.12071

Do, C., Waples, R. S., Peel, D., Macbeth, G. M., Tillett, B. J., & Ovenden, J. R. (2013). NeEstimator: re-implementation of software for the estimation of contemporary effective population size from genetic data. *Molecular Ecology Resources*, *14*(1), 209–214. https://doi.org/10.1111/1755-0998.12157

Dowling, T. E., Turner, T. F., Carson, E. W., Saltzgiver, M. J., Adams, D., Kesner, B., & Marsh, P. C. (2014). Time-series analysis reveals genetic responses to intensive management of razorback sucker (*Xyrauchen texanus*). *Evolutionary Applications*, *7*(3), 339-354. https://doi.org/10.1111/eva.12125

Dudley, R., S. Platania, and G. White. (2021). Rio Grande Silvery Minnow population monitoring during 2020. Submitted to the U.S. Bureau of Reclamation, Albuquerque, New Mexico, USA. https://doi.org/10.13140/RG.2.2.14448.79360.

Dudley, R. K., Platania, S. P., and G. C. White. (2019). Rio Grande Silvery Minnow Population Monitoring Program during 2019. Report submitted to the U.S. Bureau of Reclamation Albuquerque Office. 209 pp.

Ellegren, H. (2004). Microsatellites: simple sequences with complex evolution. Nat Rev Genet 5, 435–445 (2004). https://doi.org/10.1038/nrg1348

Fischer, M. C., Rellstab, C., Leuzinger, M., Roumet, M., Gugerli, F., Shimizu, K. K., Holderegger, R., & Widmer, A. (2017). Estimating genomic diversity and population differentiation – an empirical comparison of microsatellite and SNP variation in *Arabidopsis halleri*. *BMC Genomics*, *18*(1), 1–15. https://doi.org/10.1186/s12864-016-3459-7

Forstmeier, W., Schielzeth, H., Mueller, J. C., Ellegren, H., & Kempenaers, B. (2012). Heterozygosity–fitness correlations in zebra finches: microsatellite markers can be better than their reputation. *Molecular Ecology*, *21*(13), 3237-3249. https://doi.org/10.1111/j.1365-294X.2012.05593.x

Gilbert, K. J., & Whitlock, M. C. (2015). Evaluating methods for estimating local effective population size with and without migration. *Evolution*, *69*(8), 2154-2166. https://doi.org/10.1111/evo.12713

Gossieaux, P., Bernatchez, L., Sirois, P., & Garant, D. (2019). Impacts of stocking and its intensity on effective population size in Brook Charr (*Salvelinus fontinalis*) populations. *Conservation Genetics*, *20*(4), 729–742. https://doi.org/10.1007/s10592-019-01168-2

Guillot, G., & Foll, M. (2009). Correcting for ascertainment bias in the inference of population structure. *Bioinformatics*, *25*(4), 552-554. https://doi.org/10.1093/bioinformatics/btn665

Guo, S. W., & Thompson, E. A. (1992). Performing the exact test of Hardy-Weinberg proportion for multiple alleles. *Biometrics*, 361-372. https://doi.org/10.2307/2532296

Hedgecock, D., Launey, S., Pudovkin, A. I., Naciri, Y., Lapegue, S., & Bonhomme, F. (2007). Small effective number of parents (Nb) inferred for a naturally spawned cohort of juvenile European flat oysters *Ostrea edulis*. *Marine Biology*, *150*(6), 1173-1182. https://doi.org/10.1007/s00227-006-0441-y

Hill, W. G. (1981). Estimation of effective population size from data on linkage disequilibrium. *Genetical Research*, *38*(3), 209–216. https://doi.org/10.1017/s0016672300020553

Hoban, S., Arntzen, J. A., Bruford, M. W., Godoy, J. A., Hoelzel, A., Segelbacher, G., Vilá, C. & Bertorelle, G. (2014). Comparative evaluation of potential indicators and temporal sampling protocols for monitoring genetic erosion. *Evolutionary Applications*, *7*(9), 984-998. https://doi.org/10.1111/eva.12197

Hoffman, J. I., Simpson, F., David, P., Rijks, J. M., Kuiken, T., Thorne, M. A. S., Lacy, R. C., & Dasmahapatra, K. K. (2014). High-throughput sequencing reveals inbreeding depression in a natural population. *Proceedings of the National Academy of Sciences*, *111*(10), 3775–3780. https://doi.org/10.1073/pnas.1318945111

Horwitz, R. J., Keller, D. H., Overbeck, P. F., Platania, S. P., Dudley, R. K., & Carson, E. W. (2018). Age and Growth of the Rio Grande Silvery Minnow, an Endangered, Short-Lived Cyprinid of the North American Southwest. *Transactions of the American Fisheries Society*, *147*(2), 265–277. https://doi.org/10.1002/tafs.10012

Huisman, J., Kruuk, L. E., Ellis, P. A., Clutton-Brock, T., & Pemberton, J. M. (2016). Inbreeding depression across the lifespan in a wild mammal population. *Proceedings of the National Academy of Sciences*, *113*(13), 3585-3590. https://doi.org/10.1073/pnas.1518046113

Jombart, T., & Ahmed, I. (2011). adegenet 1.3-1: new tools for the analysis of genome-wide SNP data. *Bioinformatics*, *27*(21), 3070–3071. https://doi.org/10.1093/bioinformatics/btr521

Jones, A. T., Ovenden, J. R., & Wang, Y. G. (2016). Improved confidence intervals for the linkage disequilibrium method for estimating effective population size. *Heredity*, *117*(4), 217-223. https://doi.org/10.1038/hdy.2016.19

Jorde, P. E., & Ryman, N. (1995). Temporal allele frequency change and estimation of effective size in populations with overlapping generations. *Genetics*, *139*(2), 1077–1090. https://doi.org/10.1093/genetics/139.2.1077

Jorde, P. E., & Ryman, N. (1996). Demographic genetics of brown trout (*Salmo trutta*) and estimation of effective population size from temporal change of allele frequencies. *Genetics*, *143*(3), 1369–1381. https://doi.org/10.1093/genetics/143.3.1369

Kardos, M., Allendorf, F. W., & Luikart, G. (2014). Evaluating the role of inbreeding depression in heterozygosity-fitness correlations: how useful are tests for identity disequilibrium? *Molecular Ecology Resources*, *14*(3), 519-530. https://doi.org/10.1111/1755-0998.12193

Kardos, M., Åkesson, M., Fountain, T., Flagstad, Ø., Liberg, O., Olason, P., Sand, H., Wabakken, P., Wikenros, C. & Ellegren, H. (2018). Genomic consequences of intensive inbreeding in an isolated wolf population. *Nature Ecology & Evolution*, *2*(1), 124-131. https://doi.org/10.1038/s41559-017-0375-4

Kassambara, A. and M.A. Kassambara. 2020. R Package *ggpubr*.

Keenan, K., McGinnity, P., Cross, T. F., Crozier, W. W., & Prodöhl, P. A. (2013). diveRsity: An R package for the estimation and exploration of population genetics parameters and their associated errors. *Methods in Ecology and Evolution*, *4*(8), 782–788. https://doi.org/10.1111/2041-210x.12067

Keller, M. C., Visscher, P. M., & Goddard, M. E. (2011). Quantification of inbreeding due to distant ancestors and its detection using dense single nucleotide polymorphism data. *Genetics*, *189*(1), 237–249. https://doi.org/10.1534/genetics.111.130922

Koelewijn, H.P., Pérez-Haro, M., Jansman, H.A.H., Boerwinkel, M.C., Bovenschen, J., Lammertsma, D.R., Niewold, F.J.J. and Kuiters, A.T. (2010). The reintroduction of the Eurasian otter (Lutra lutra) into the Netherlands: hidden life revealed by noninvasive genetic monitoring. *Conservation Genetics*, *11*(2), 601-614. https://doi.org/10.1007/s10592-010-0051-6

Lehnert, S. J., DiBacco, C., Jeffery, N. W., Blakeslee, A. M. H., Isaksson, J., Roman, J., Wringe, B. F., Stanley, R. R. E., Matheson, K., McKenzie, C. H., Hamilton, L. C., & Bradbury, I. R. (2018). Temporal dynamics of genetic clines of invasive European green crab (*Carcinus maenas*) in eastern North America. *Evolutionary Applications*, *11*(9), 1656–1670. https://doi.org/10.1111/eva.12657

Lemopoulos, A., Prokkola, J. M., Uusi-Heikkilä, S., Vasemägi, A., Huusko, A., Hyvärinen, P., Koljonen, M., Koskiniemi, J., & Vainikka, A. (2019). Comparing RADseq and microsatellites for estimating genetic diversity and relatedness — Implications for brown trout conservation. *Ecology and Evolution*, *9*(4), 2106–2120. https://doi.org/10.1002/ece3.4905

Liaw, A., Wiener, M. (2002). Classification and regression by random forest. *R news*, *2,*18-22.

Ljungqvist, M., Åkesson, M., & Hansson, B. (2010). Do microsatellites reflect genome-wide genetic diversity in natural populations? A comment on Väli et al. (2008).

Lyubchich, V., Gel, Y. R., Brenning, A., Chu, C., Huang, X., Islambekov, U., ... & Lyubchich, M. V. (2022). Package 'funtimes'.

Mann, H. B. (1945). Nonparametric Tests Against Trend. *Econometrica*, *13*(3), 245. https://doi.org/10.2307/1907187

Marandel, F., Charrier, G., Lamy, J. B., Le Cam, S., Lorance, P., & Trenkel, V. M. (2020). Estimating effective population size using RADseq: Effects of SNP selection and sample size. *Ecology and Evolution*, *10*(4), 1929-1937. https://doi.org/10.1002/ece3.6016

McLennan, E. A., Wright, B. R., Belov, K., Hogg, C. J., & Grueber, C. E. (2019). Too much of a good thing? Finding the most informative genetic data set to answer conservation questions. *Molecular Ecology Resources*, *19*(3), 659–671. https://doi.org/10.1111/1755-0998.12997

Meirmans, P. G. (2020). genodive version 3.0: Easy-to-use software for the analysis of genetic data of diploids and polyploids. *Molecular Ecology Resources*, *20*(4), 1126-1131. https://doi.org/10.1111/1755-0998.13145

Miller, J. M., & Coltman, D. W. (2014). Assessment of identity disequilibrium and its relation to empirical heterozygosity fitness correlations: a meta-analysis. *Molecular Ecology*, *23*(8), 1899-1909. https://doi.org/10.1111/mec.12707

Miller, J. M., Cullingham, C. I., & Peery, R. M. (2020). The influence of a priori grouping on inference of genetic clusters: simulation study and literature review of the DAPC method. *Heredity*, *125*(5), 269-280. https://doi.org/10.5061/dryad.4tmpg4f76

Miller, J. M., Malenfant, R. M., David, P., Davis, C. S., Poissant, J., Hogg, J. T., Festa-Bianchet, M., & Coltman, D. W. (2014). Estimating genome-wide heterozygosity: effects of demographic history and marker type. *Heredity*, *112*(3), 240–247. https://doi.org/10.1038/hdy.2013.99

Nei, M. (1987). *Molecular evolutionary genetics*. Columbia University Press.

Nei, M., & Tajima, F. (1981). Genetic drift and estimation of effective population size. *Genetics*, *98*(3), 625–640. https://doi.org/10.1093/genetics/98.3.625

Ohta, T., & Cockerham, C. C. (1974). Detrimental genes with partial selfing and effects on a neutral locus. *Genetics Research*, *23*(2), 191-200. https://doi:10.1017/S0016672300014816

Osborne, M. J., Carson, E. W., & Turner, T. F. (2012). Genetic monitoring and complex population dynamics: insights from a 12-year study of the Rio Grande silvery minnow. *Evolutionary Applications*, *5*(6), 553–574. https://doi.org/10.1111/j.1752-4571.2011.00235.x

Osborne, M. J., Dowling, T. E., Scribner, K. T., & Turner, T. F. (2020). Wild at heart: Programs to diminish negative ecological and evolutionary effects of conservation hatcheries. *Biological Conservation*, *251*, 108768. https://doi.org/10.1016/j.biocon.2020.108768

Osborne, M. J., Perez, T. L., Altenbach, C. S., & Turner, T. F. (2013). Genetic analysis of captive spawning strategies for the endangered Rio Grande silvery minnow. *Journal of Heredity*, *104*(3), 437–446. https://doi.org/10.1093/jhered/est013

Osborne, M. J., Benavides, M. A., Alò, D., & Turner, T. F. (2006). Genetic effects of hatchery propagation and rearing in the endangered Rio Grande silvery minnow, *Hybognathus amarus*. *Reviews in Fisheries Science*, *14*(1-2), 127-138. https://doi.org/10.1080/10641260500341544

Osborne, M. J., Benavides, M. A., & Turner, T. F. (2005). Genetic heterogeneity among pelagic egg samples and variance in reproductive success in an endangered freshwater fish, *Hybognathus amarus* (Cyprinidae). *Environmental Biology of Fishes*, *73*(4), 463-472. https://doi.org/10.1007/s10641-005-3215-3

Pflieger, W. L. (1980). *Hybognathus nuchalis* Agassiz, Central silvery minnow. *Atlas of North American Freshwater Fishes*:*867*.

Platania, S. P. (1993). The fishes of the Rio Grande between Velarde and Elephant Butte Reservoir and their habitat associations. *Report to the New Mexico Department of Game and Fish, Santa Fe, and US Bureau of Reclamation (Albuquerque Projects Office), Albuquerque, NM*, *188*.

905 Pohlert, T. (2020) Package "*Trend*": Non-Parametric Trend Tests and Change-Point Detection
906 vers. 1.1.4. R Package, 26.
907 RStudio Team (2019). RStudio: Integrated Development Environment for R.
908 R Core Team. (2019). R: A language and environment for statistical computing. R Foundation
909 for Statistical Computing, Vienna, Austria. URL https://www.R-project.org/
910 Rice, W. R. (1989). Analyzing tables of statistical tests. *Evolution*, *43*(1), 223-225. https://doi.org/
911 10.2307/2409177
912 Robinson, S. P., Simmons, L. W., & Kennington, W. J. (2013). Estimating relatedness and
913 inbreeding using molecular markers and pedigrees: the effect of demographic history.
914 *Molecular Ecology*, *22*(23), 5779–5792. https://doi.org/10.1111/mec.12529
915 Robertson, A. (1965). The interpretation of genotypic ratios in domestic animal populations.
916 *Animal Science*, *7*(3), 319-324. https://doi.org/10.1017/S0003356100025770
917 Roesti, M., Hendry, A. P., Salzburger, W., & Berner, D. (2012). Genome divergence during
918 evolutionary diversification as revealed in replicate lake–stream stickleback population
919 pairs. *Molecular ecology*, *21*(12), 2852-2862. https://doi.org/10.1111/j.1365-
920 294X.2012.05509.x
921 Rosner, B. (1983). Percentage Points for a Generalized ESD Many-Outlier Procedure.
922 *Technometrics*, *25*, 165-172.
923 Rousset, F. (2008). genepop'007: a complete re-implementation of the genepop software for
924 Windows and Linux. *Molecular ecology resources*, *8*(1), 103-106.
925 https://doi.org/10.1111/j.1471-8286.2007.01931.x
926 Russello, M. A., Waterhouse, M. D., Etter, P. D., & Johnson, E. A. (2015). From promise to
927 practice: pairing non-invasive sampling with genomics in conservation. *PeerJ*, *3*, e1106.
928 https://doi.org/10.7717/peerj.1106
929 Schwartz, M., Luikart, G., & Waples, R. (2007). Genetic monitoring as a promising tool for
930 conservation and management. *Trends in Ecology & Evolution*, *22*(1), 25–33.
931 https://doi.org/10.1016/j.tree.2006.08.009
932 Sen, P. K. (1968). Estimates of the Regression Coefficient Based on Kendall's Tau. *Journal of*
933 *the American Statistical Association*, *63*(324), 1379–1389.
934 https://doi.org/10.1080/01621459.1968.10480934
935 Sin, S. Y. W., Hoover, B. A., Nevitt, G. A., & Edwards, S. V. (2021). Demographic History, Not
936 Mating System, Explains Signatures of Inbreeding and Inbreeding Depression in a Large
937 Outbred Population. *The American Naturalist*, *197*(6), 658–676.
938 https://doi.org/10.1086/714079
939 Stoffel, M. A., Esser, M., Kardos, M., Humble, E., Nichols, H., David, P., & Hoffman, J. I.
940 (2016). inbreedR: an R package for the analysis of inbreeding based on genetic markers.
941 *Methods in Ecology and Evolution*, *7*(11), 1331-1339. https://doi.org/10.1111/2041-
942 210X.12588
943 Sunde, J., Yıldırım, Y., Tibblin, P., & Forsman, A. (2020). Comparing the performance of
944 microsatellites and RADseq in population genetic studies: Analysis of data for pike (*Esox*
945 *lucius*) and a synthesis of previous studies. *Frontiers in Genetics*, *11*, 218.
946 https://doi.org/10.3389/fgene.2020.00218
947 Szulkin, M., Bierne, N., & David, P. (2010). Heterozygosity-fitness correlations: A time for
948 reappraisal. *Evolution*, *64*, 1202–1217. https://doi.org/10.1111/j.1558-5646.2010.00966.x

949 Townsend, S. M., & Jamieson, I. G. (2013). Molecular and pedigree measures of relatedness
950 provide similar estimates of inbreeding depression in a bottlenecked population. *Journal of*
951 *Evolutionary Biology*, *26*(4), 889–899. https://doi.org/10.1111/jeb.12109
952 Tsitrone, A., Rousset, F., & David, P. (2001). Heterosis, Marker Mutational Processes and
953 Population Inbreeding History. *Genetics*, *159*(4), 1845–1859.
954 https://doi.org/10.1093/genetics/159.4.1845
955 Turner, T. F., Osborne, M. J., Moyer, G. R., Benavides, M. A., & Alò, D. (2006). Life history
956 and environmental variation interact to determine effective population to census size ratio.
957 *Proceedings of the Royal Society B: Biological Sciences*, *273*(1605), 3065–3073.
958 https://doi.org/10.1098/rspb.2006.3677
959 Turner, T. F., Salter, L. A., & Gold, J. R. (2001). Temporal-method estimates of Ne from highly
960 polymorphic loci. *Conservation Genetics*, *2*(4), 297–308.
961 https://doi.org/10.1023/a:1012538611944
962 U.S. Fish and Wildlife Service. (1994). Endangered and threatened wildlife and plants: final rule
963 to list the Rio Grande silvery minnow as an endangered species. *Federal Register*, 59,
964 36988–36995.
965 U. S. Fish and Wildlife Service. (2018a). Rio Grande Silvery Minnow genetics and propagation
966 management plan, 2018 revision: Albuquerque, New Mexico.
967 U.S. Fish and Wildlife Service. Rio Grande Silvery Minnow Genetic Management and Captive
968 Propagation Workgroup. (2018b). Rio Grande silvery minnow annual augmentation plan,
969 2018-2022.
970 Väli, L., Einarsson, A., Waits, L., & Ellegren, H. (2008). To what extent do microsatellite
971 markers reflect genome-wide genetic diversity in natural populations? *Molecular Ecology*,
972 *17*(17), 3808–3817. https://doi.org/10.1111/j.1365-294x.2008.03876.x
973 Vendrami, D. L. J., de Noia, M., Telesca, L., Brodte, E., & Hoffman, J. I. (2020). Genome-wide
974 insights into introgression and its consequences for genome-wide heterozygosity in the
975 *Mytilus* species complex across Europe. *Evolutionary Applications*, *13*(8), 2130–2142.
976 https://doi.org/10.1111/eva.12974
977 Wang, L., M. G. Akritas, and I. Van Keilegom. (2008). An ANOVA-type Nonparametric
978 diagnostic test for heteroscedastic regression models. *Journal of Nonparametric Statistics*
979 20 (5), 365–382.
980 Wang, J. (2011). A new likelihood estimator and its comparison with moment estimators of
981 individual genome-wide diversity. *Heredity*, *107*(5), 433-443.
982 https://doi.org/10.1038/hdy.2011.30
983 Wang, J. (2021). EMIBD9 software. Available at: https://www.zsl.org/science/software/emibd9
984 Waples, R. S. (1989). A generalized approach for estimating effective population size from
985 temporal changes in allele frequency. *Genetics*, *121*(2), 379–391.
986 https://doi.org/10.1093/genetics/121.2.379
987 Waples, R. S. (2005). Genetic estimates of contemporary effective population size: to what time
988 periods do the estimates apply? *Molecular Ecology*, *14*(11), 3335–3352.
989 https://doi.org/10.1111/j.1365-294x.2005.02673.x
990 Waples, R. S. (2015). Testing for Hardy–Weinberg proportions: have we lost the plot?. *Journal*
991 *of Heredity*, *106*(1), 1-19. https://doi.org/10.1093/jhered/esu062
992 Waples, R. S., & Do, C. (2010). Linkage disequilibrium estimates of contemporary NeV using
993 highly variable genetic markers: A largely untapped resource for applied conservation and

evolution. *Evolutionary Applications*, *3*(3), 244–262. https://doi.org/10.1111/j.1752-4571.2009.00104.x

Weir, B. S., & Cockerham, C. C. (1984). Estimating F-statistics for the analysis of population structure. *Evolution*, 1358-1370. https://doi.org/10.2307/2408641

Whitlock, M. C. (2011). G'($_{ST}$) and D do not replace F_{ST}. *Molecular Ecology*, *20*(6), 1083-1091. https://doi.org/10.1111/j.1365-294X.2010.04996.x

Wright, S. (1922). Coefficients of inbreeding and relationship. *The American Naturalist*, *56*(645), 330-338.

Wright, S. (1950). Genetical structure of populations. *Nature*, *166*, 247-49.

Yackulic, C., Archdeacon, T., Valdez, R., Hobbs, M., Porter, M., Lusk, J., Tanner, A., Gonzales, E., Lee, D. and Haggerty. G. (2022). Quantifying flow and nonflow management impacts on an endangered fish by integrating, data, research, and expert opinion. *Ecosphere,* In Press.

Zimmerman, S. J., Aldridge, C. L., & Oyler-McCance, S. J. (2020). An empirical comparison of population genetic analyses using microsatellite and SNP data for a species of conservation concern. *BMC genomics*, *21*(1), 1-16. https://doi.org/10.1186/s12864-020-06783-9

Table 1 Temporal and spatial origin of Rio Grande silvery minnow samples for SNP discovery. Asterisks denote tissue samples (frozen and ethanol). All other samples were purified from previous DNA isolations. The total number of samples was 379 (13 samples were later discarded because of missing data). Analyses were based on total number of samples per year, since there is no evidence of population structure between river reaches (Osborne et al. 2012).

River Reach	**1999**	**2000**	**2002**	**2004**	**2006**	**2008**	**2009**	**2010**	**2012**	**2015**	**2017**	**2018**
Angostura	--	--	9	9	10*	10*	10*	9*	10	11*	10*	10*
Isleta	--	--	11	11	10*	10*	--	10*	11	11*	10*	10*
San Acacia	30*	42*	10	6	10*	10*	20*	10*	9	9*	10*	20*
Total	30	42	30	28	30	30	30	29	30	31	30	40

Table 2 Description of statistics used to measure inbreeding/identity disequilibrium.

Symbol	Statistic	Description	Reference
$\hat{g}_2$	Identity disequilibrium	• Low-bias estimate of g_2. Measures excess of double heterozygotes at two loci relative to expectations (equation 8 in David et al. 2007).	David et al. 2007
sMLH	Standardized multilocus heterozygosity	• Mean heterozygosity across all genotyped loci divided by mean heterozygosity at loci genotyped in the population (i.e., temporal sample). Standardizes heterozygosity when not all loci are typed in each individual.	Coltman et al. 1999
IR	Internal relatedness	• IR=(2H-$\sum$f*i*)/ (2N- $\sum$f*i*) where H is the number of homozygous loci and N is the number if loci and f*i* is the frequency of the i^{th} allele in the genotype. Weights rare alleles more heavily.	Amos et al. 2001
F_{IS}	Fixation index	• Inbreeding at the population level with respect to nonrandom mating within demes. Measures heterozygote deficiency/excess per locus. $F_{IS}=\frac{Hexp-Hobs}{Hexp}$	Wright 1951
F	IBD inbreeding	• F calculated by EMIBD is derived from estimates of the 9 condensed IBD coefficients between two individuals. $\bar{F}$ is the average F for each individual. $\bar{F}_{pop}$- population average.	Wang 2021

Table 3 Pearson correlation coefficients for genetic metrics (unbiased gene diversity [*u*Hs], observed heterozygosity [H_O], allelic richness [A_R], average inbreeding coefficient [F_{IS}], variance effective population size (N_{eV}), and Mantel correlation for G''_{ST} and Spearman correlation for linkage disequilibrium effective population size (N_{eD}) and calculated between microhaplotypes and microsatellites and associated *p*-values.

Metric	**Correlation**	***p*-value**
uH_S	-0.22	0.490
H_O	0.190	0.550
A_R	-0.70	0.012*
F_{IS}	0.230	0.480
N_{eV}	0.136	0.689
G''_{ST}	0.153	0.023*
N_{eD}	0.680	0.016*

Table 4 Summary of differences/similarities of genetic metrics between datasets and broad conclusions.

	Genetic Metric	Microsatellites	Microhaplotypes	Conclusions
Individual metrics	sMLH/IR/$\overline{F}$	Strong correlation between sMLH and IBD $\overline{F}$	Strong correlation between sMLH and IBD $\overline{F}$	sMLH/IR- reflect IBD $\overline{F}$. Microhaplotypes detect temporal changes in individual diversity.
	$\hat{g}_2$ /$\overline{F}_{pop}$	Wide CIs for sample Most $\hat{g}_2$ estimates not >0	Narrow CIs. $\hat{g}_2$ >0	Microsatellites lack power to estimate inbreeding/ID via $\hat{g}_2$ in most cases. Temporal changes in inbreeding ($g_2/\overline{F}_{pop}$) detected across time series by microhaplotypes.
Population metrics	(uH$_E$, H$_O$, F$_{IS}$, A$_R$)	Overlapping CIs No trend apparent for uH$_E$, H$_O$, F$_{IS}$. Reduced A$_R$ in some years corresponding to reduced abundance	Narrow CIs, increased precision Years with increased values of F$_{IS}$	Temporal patterns differ, but both dataset show genetic diversity maintained. Increased precision of microhaplotype-based estimates allows small differences between temporal samples to be detected (i.e., F$_{IS}$ and H$_O$).
Temporal divergence	DAPC	Weak temporal divergence	Temporal divergence between old and more recent samples	Temporal shift in allele frequencies detected from microhaplotypes.
	F$_{ST}$	Range: 0.003-0.017/ Smaller CIs	Range: -0.0006-0.006 Overlapping CIs	Strongly correlated. Small degree of divergence between temporal collections.
	Mean F$_{ST}$	0.006	0.002	Smaller values for microhaplotype-based estimates.
Effective population size	N$_{eV}$	N$_{eV}$=33-604 Overlapping CIs	N$_{eV}$=122 - 576 Narrow CIs, increased precision	N$_{eV}$ is small. Both datasets show an increase in N$_{eV}$ for 2015-2017 and decrease between 2017-2018. Differences between N$_{eV}$ estimates can be identified with microhaplotypes.
	N$_{eD}$	Wide CIs N$_{eD}$=489 – 12,127	Wide CIs N$_{eD}$=731-3,579	Strongly correlated. Both datasets detect an order of magnitude decline associated with population collapse in 2012-2014.

Table 5 A comparison of key findings and recommendations based on microsatellite data and microhaplotype data for Rio Grande Silvery Minnow. Hypothesized biological processes that underlie key findings are listed, as are management recommendations that emerged from key findings. References are provided for microsatellite data. Inferences based on microhaplotypes are described in the text.

Key Finding	Micro-satellites	Micro-haplotypes	Underlying Biological Process	Management Recommendations
Genetic diversity metrics stable over a 20-year time series	yes	yes [a]	Sufficient diversity remains in wild and hatchery stocks to maintain 'neutral' genetic diversity despite large population fluctuations.	The comprehensive adaptive management strategy is meeting many targets for 'neutral' genetic diversity.[1, 2]
Low A_R in some captive brood stocks	yes	not tested [b]	Too few captive spawners to form a representative brood stock.	Increase broodstock numbers, spawning, and rearing capacity in multiple facilities.[3]
Inbreeding trends detected?	no	yes	Microhaplotypes have more power to detect inbreeding but further evaluation is necessary.	Increase broodstock numbers, spawning, and rearing capacity in multiple facilities.
Wild-caught drifting eggs (WCE) sufficiently represent whole-population genetic diversity	yes	not tested	Spawning is triggered by spring snowmelt flow pulse, eggs drift downstream. Multiple flow peaks initiate multiple spawning events.	Temporal sampling interval should span the entire spawning season. Eggs should be collected from all river reaches. WCE prioritized for augmentation and refugial broodstock. [2, 4, 5]

$F_{ST} \approx 0$ across Rio Grande sampling localities	yes	not tested	High dispersal and gene flow throughout the current species range. Downstream-biased egg and larval dispersal.	Collect broodstock from all river reaches (i.e., the species range) to maximize diversity. It is not necessary to create geographically distinct stocks. [1, 4, 6, 7]
$N_e/N << 0.1$ in wild populations	yes	yes	Downstream transport of pelagic eggs past dams introduces high variance in reproductive success (VRS) among spawning aggregates. Other species exhibit $N_e/N \geq 0.1$.	Re-engineer dam and diversion structures to allow for upstream fish passage. Restore connectivity to lateral floodplain habitat to enhance egg retention and recruitment. [1, 4, 6, 7]
N_{eV} is not correlated with N in wild populations	yes	not tested [d]	Inputs from the hatchery and VRS strongly influence the relationship of N_e and N.	N_e is not a proxy for wild abundance. Demographic and genetic monitoring are required to evaluate ecological and evolutionary effects of population fluctuation and hatchery inputs. [1, 7, 8]

[1] Osborne et al. 2012, [2] Osborne et al. 2020, [3] Osborne et al. 2006, [4] Osborne et al. 2005, [5] USFWS 2018a,[6] Alò & Turner 2005,[7] Turner et al. 2006 [8] Carson et al. 2020

[a] Not all metrics perform equally well across marker classes (see text).
[b] Not explicitly tested, but A_R is not an effective metric for microhaplotype data.
[c] Microhaplotypes are more sensitive to inbreeding effects or have more power to detect them.
[d] Not tested.

Figure 1. Summary of the of the main demographic events and management actions since the beginning of genetic monitoring of Rio Grande silvery minnow. This species was listed under the Endangered Species Act in 1994. Genetic monitoring (GM) commenced in 1999 and has continued annually since (except for 2013-2014 when insufficient samples were available for genetic analysis). A captive breeding and rearing program commenced on a limited scale in 2002 and in 2003 transitioned to a full-scale program with the founding of the captive population from 922,000 eggs from natural reproduction of the middle Rio Grande population (indicated by the purple arrow). The population has been augmented nearly every year since. Samples used for SNP discovery are indicated by the red arrows. Population bottlenecks are indicated by the red bars. N-estimated wild-born and augmented Rio Grande silvery minnow from Yackulic et al. (In Press).

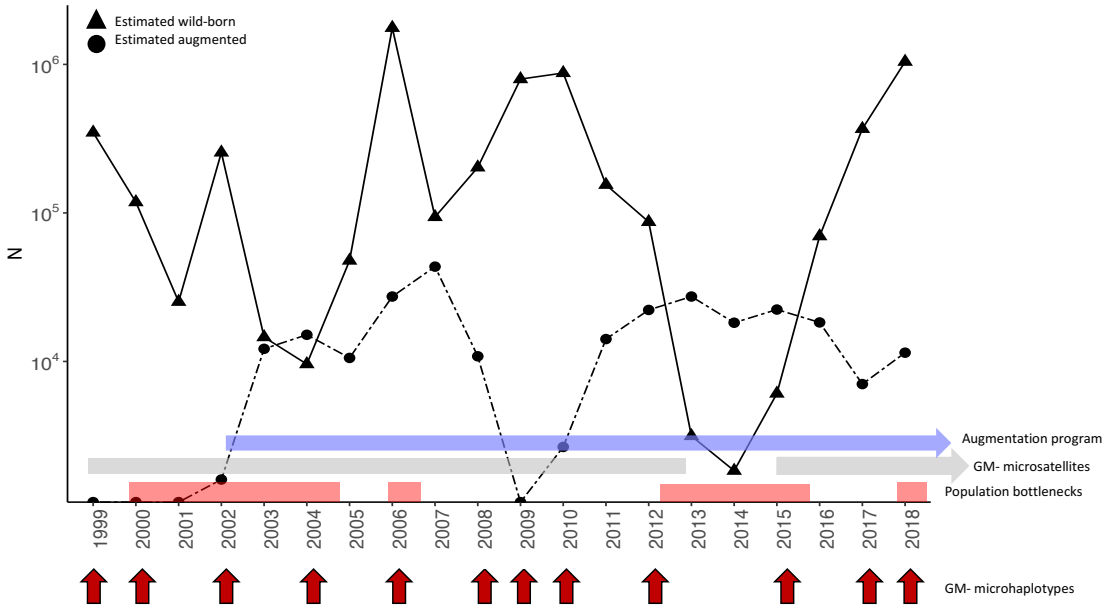

Figure 2. Genetic diversity estimates across temporal collections: **a**) unbiased heterozygosity (uH_S), **b**) observed heterozygosity (H_O) and **c**) allelic richness (A_R) based on microhaplotype and microsatellite (**d-f**) datasets. Note that the Y-axis scales are different. For uH_S and H_O the 95% confidence intervals are shown.

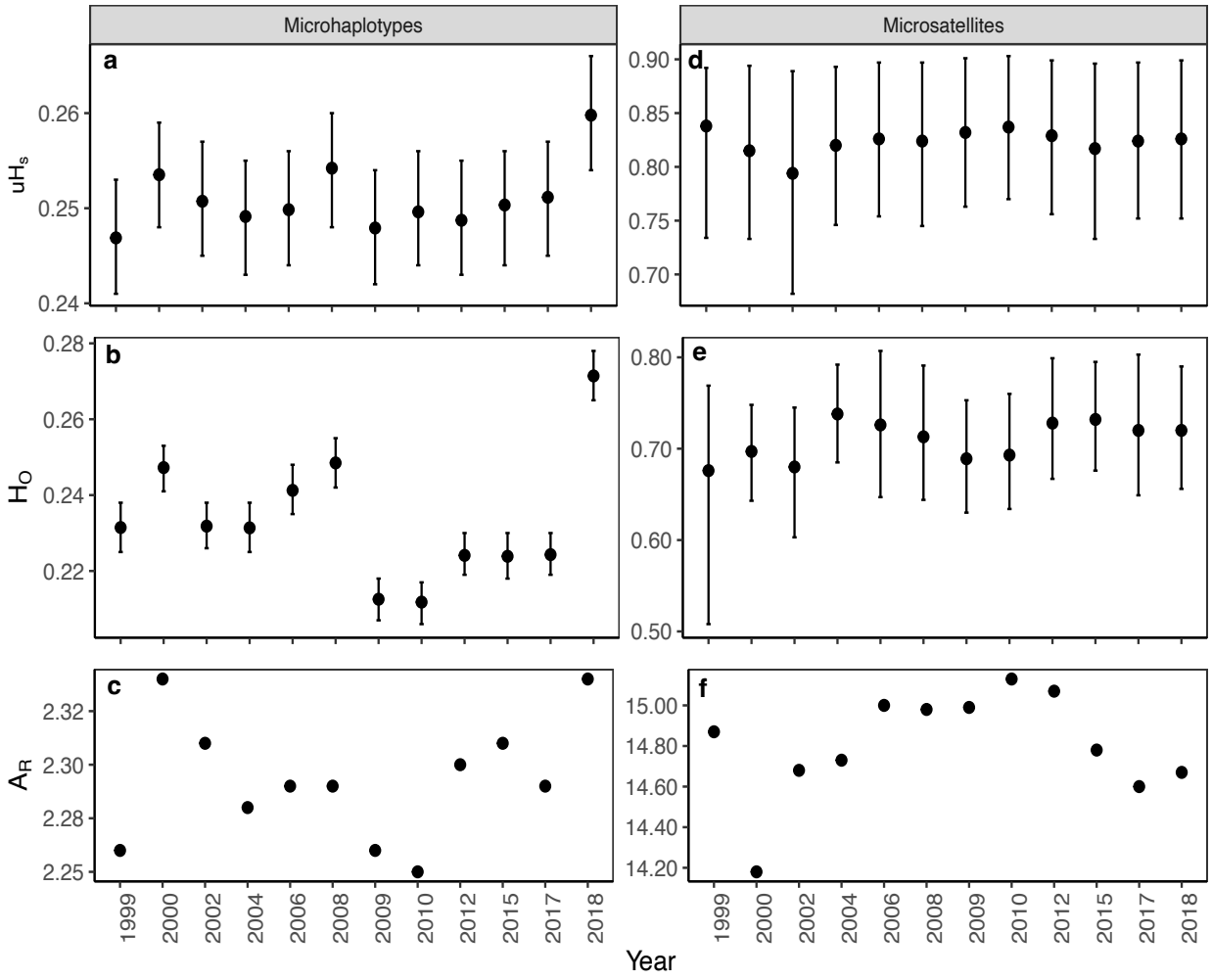

Figure 3. Genetic effective population size results based on linkage disequilibrium (N_{eD}) calculated from **a**) microhaplotypes and **b**) microsatellites and associated 95% confidence intervals. Y-axis is a log scale. Genetic effective population size results based on the variance of allele frequencies (N_{eV}) calculated from microhaplotypes (**c**) and microsatellites (**d**) using the method of Nei and Tajima (1989) and associated 95% confidence intervals.

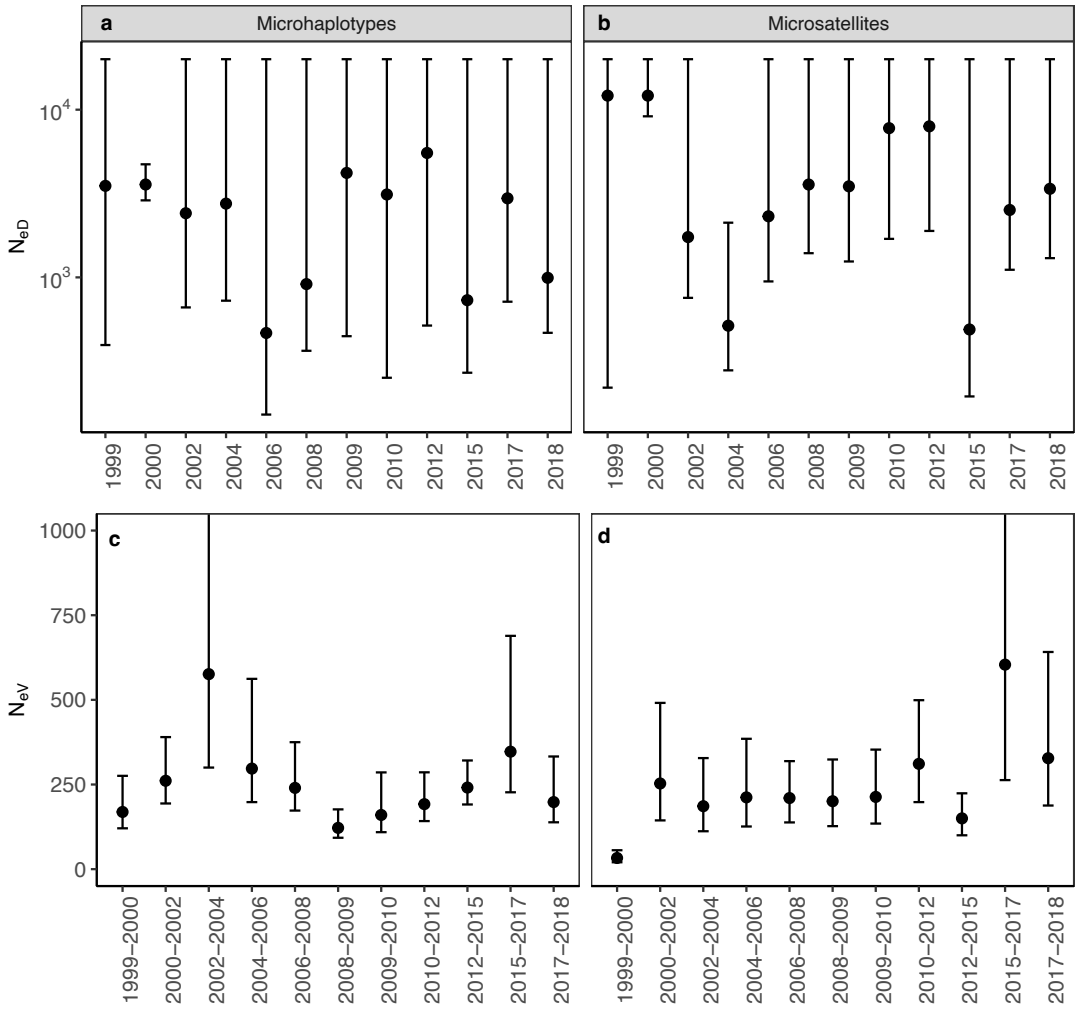

Figure 4. Results of discriminant analysis of principal components (DAPC) based on **a)** microhaplotypes and **b)** microsatellite data. In each panel the curves represent the density of individuals across the first discriminant function (DF) axis. The first DF axis explained 35% of the variance for microhaplotypes and 37% of the variance for microsatellites. The inset in each panel shows the ellipses representing the 95% confidence level for a multivariate normal distribution, plotted on the first and second DF axes. Colors represent temporal samples.

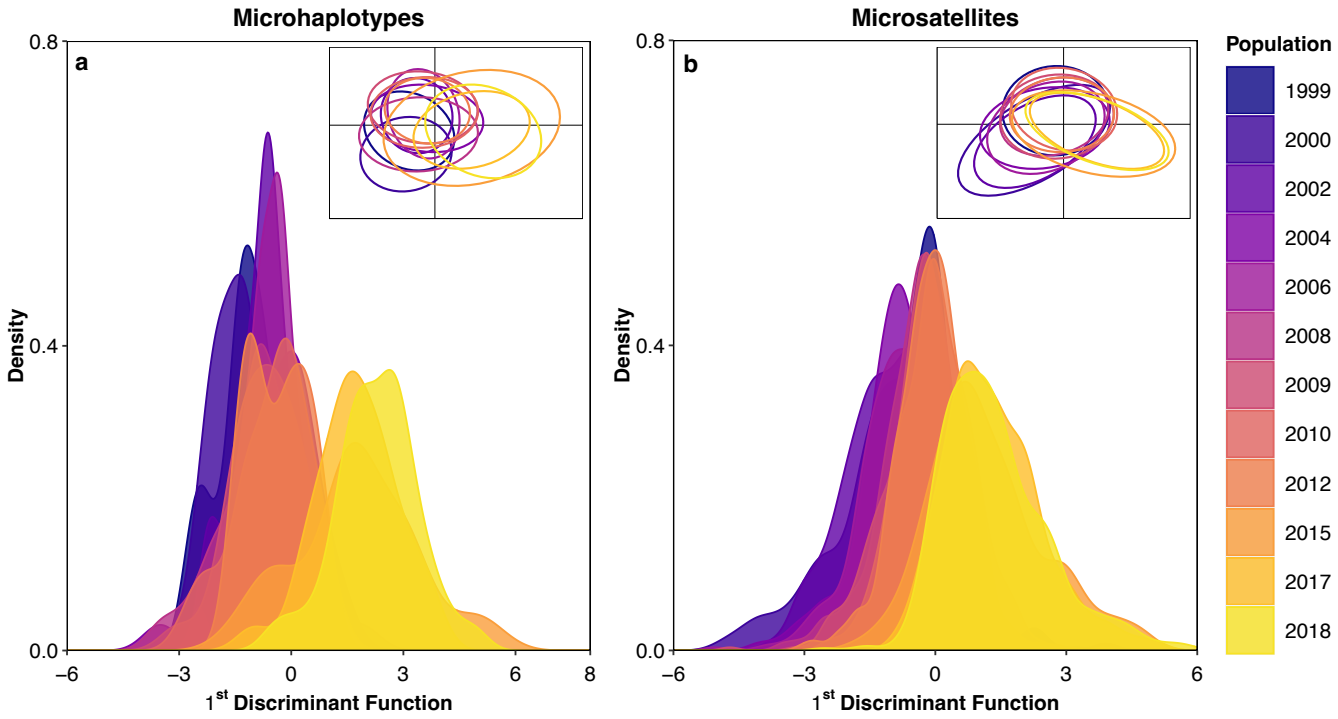

Figure 5 a) Mean standardized multilocus heterozygosity (sMLH) and **b**) mean internal relatedness (IR) for temporal samples based on microhaplotypes, and **c**, **d**) microsatellites.

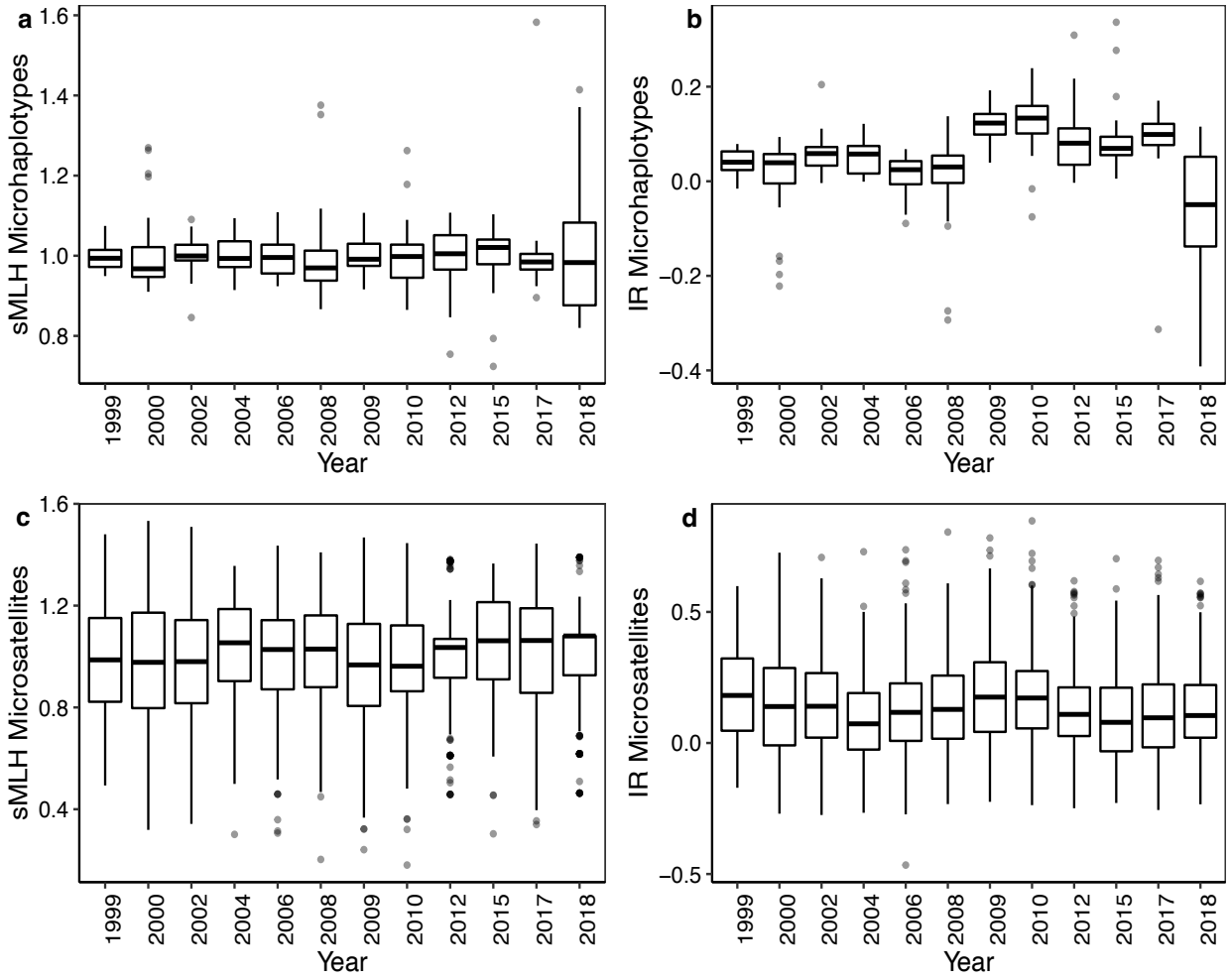

Figure 6. Correlation between **a**) standardized multilocus heterozygosity (sMLH) and **b**) internal relatedness (IR) and identity by descent inbreeding co-efficient $\overline{F}$ for microhaplotypes, and **c**, **d**) same metrics based on microsatellites. Pearson correlation co-efficient (r), r^2 values and p-values are shown on each plot.

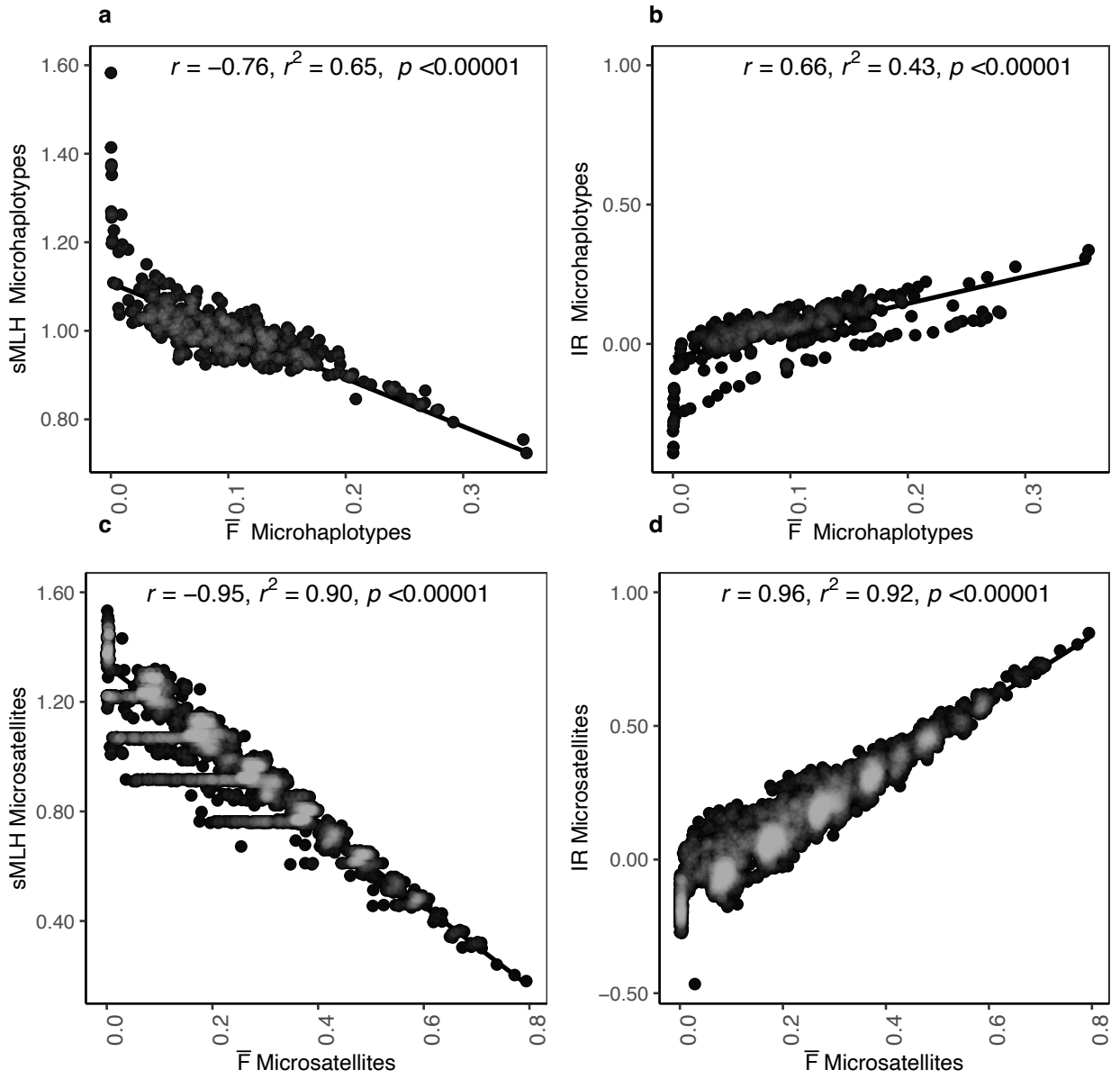

Figure 7 a) average IBD $\bar{F}_{pop}$ **b**) Identity disequilibrium ($\hat{g}_2$), and **c**) F_{IS} for temporal samples based on microhaplotypes, and **d**, **e**, **f**) and microsatellites. Associated 95% confidence intervals are shown for $\hat{g}_2$ and F_{IS}, and standard deviation is given for $\bar{F}_{pop}$. The WAVK test statistics (*wk*) and p-values are shown for non-significant tests. Mann-Kendall's τ and p-values, and change-points (cp) are shown when significant monotonic trends were detected.

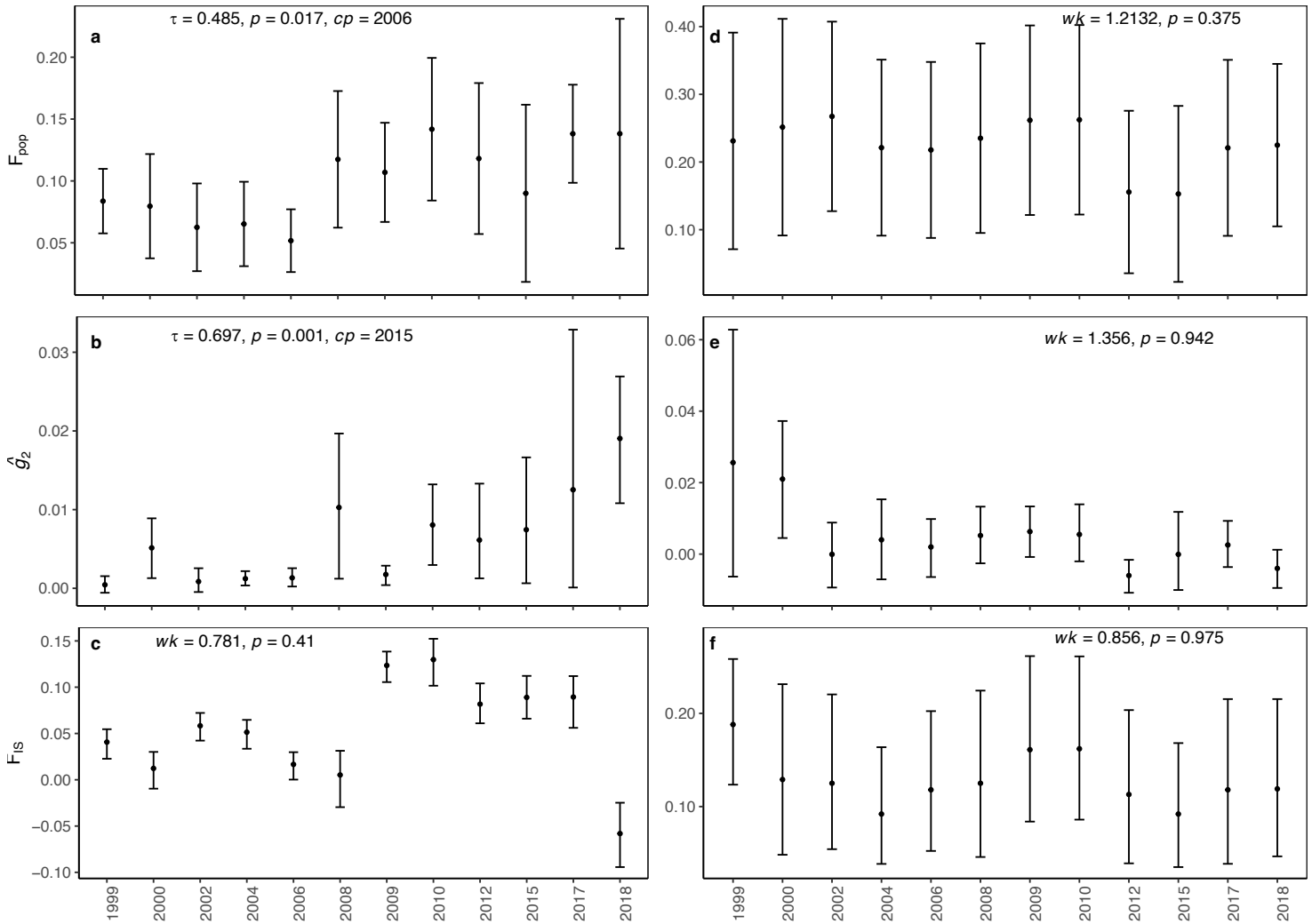
a
τ = 0.485, p = 0.017, cp = 2006
F_pop
b
τ = 0.697, p = 0.001, cp = 2015
ĝ2
c
wk = 0.781, p = 0.41
F_IS
d
wk = 1.2132, p = 0.375
e
wk = 1.356, p = 0.942
f
wk = 0.856, p = 0.975
1999
2000
2002
2004
2006
2008
2009
2010
2012
2015
2017
2018

Figure 8. Values of $\bar{F}$ and standard deviation of the mean for individuals by year based on **a**) microhaplotypes and **b**) microsatellites.